Intermediaries in phosphotransfer: structural features discriminating hybrid histidine kinase Rec domains from response regulator homologs

Mitchell Brüderlin[1], Raphael Böhm[1], Sebastian Hiller[1], Tilman Schirmer[1*] and Badri N. Dubey[1,2*]

[1] Structural Biology, Biozentrum, University of Basel, Spitalstr. 41, 4056 Basel, Switzerland
[2]CSSB Centre for Structural Systems Biology, Deutsches Elektronen-Synchrotron DESY, 22607, Hamburg, Germany

Correspondence: tilman.schirmer@unibas.ch, badri.nath.dubey@desy.de

Keywords: C-di-GMP, second messenger, cell cycle, hybrid histidine kinase, CckA, ChpT, CtrA phosphorelay, receiver domain, FATGUY motif and two-component regulatory systems

Abstract

In two-component systems, the information gathered by the histidine kinase (HK) is relayed to the cognate response regulator (RR). Thereby, the phosphoryl group of the auto-phosphorylated HK is transferred to the receiver domain of the RR to allosterically activate its effector domain. In contrast, multi-step phosphorelays comprise at least one additional Rec domain (Rec_{inter}) that is part of the HK and acts as an intermediary for phosphoryl-shuttling. While RR Rec domains have been studied extensively, little is known about Rec_{inter} domains and their potentially discriminating features. As a bona-fide Rec_{inter} domain, here we have studied the C-terminal Rec domain of the hybrid HK CckA ($CckA^{Rec}$) from *Caulobacter crescentus* by X-ray crystallography and NMR spectroscopy. $CckA^{Rec}$ exhibits the canonical Rec-fold, though with a degenerated α4 helix, in which all active site residues are pre-arranged for phosphoryl-binding. BeF_3^- binding does not alter secondary structure nor the oligomeric state, indicating the absence of allosteric changes, the hall mark of RRs. Based on structural modeling and sequence co-variation analysis, we present a detailed picture for the intra-molecular association of the CckA DHp/Rec domains and discuss the role of a FATGUY motif, a distinguishing feature of $CckA^{Rec}$ orthologs.

Introduction

Kinases constitute central cellular switches in all domains of life. Precise control of their activity in time and space is vital for the implementation of specific cellular programs. Bacteria sense and respond to a wide variety of signals through a complex network of signaling systems such as two-component system (TCS) pathways. TCSs constitute the major signal transduction system to regulate vital processes such as chemotaxis, cell cycle, virulence, etc., in response to external and endogenous stimuli. A chemical or physical input signal is perceived by the input domain of a sensory histidine kinase (HK), causing auto-phosphorylation of its conserved histidine on the DHp transmitter domain (Fig. 1A). This is followed by phosphotransfer to the conserved aspartate of the receiver (Rec) domain of a cognate response regulator (RR) to activate its effector domain to finally elicit the output[1]. Typically, effector domains regulate transcription (e.g., PhoB, OmpR) or enzymatic activity (CheB, HK, PleD), for a review see Galperin, 2010[2]. Rec domains of transcriptional regulators have been studied extensively. In the OmpR family, phosphorylation-induced Rec dimerization mediated by Y/T coupling enables DNA binding and, thus, transcriptional control[1].

For the Rec-controlled diguanylate cyclase DgcR, a change in the preformed dimeric coiled-coil association of the C-terminal Rec helices has been reported recently as the basis of activation[3]. Multi-step phosphorelays are more complex involving at least one additional Rec domain and a histidine-containing phosphotransfer (HPt) protein, both of which act as intermediaries in the phosphotransfer[1,4]. Often, the additional Rec domain is fused C-terminally to the HK to form a hybrid histidine kinase (HHK) (Fig. 1B). Multi-step phosphorelays comprise two types of Rec domains that can be distinguished functionally: (1) Rec domains that act as intermediaries in the phosphotransfer chain by shuttling the phosphoryl between HHK and HPt transmitter domains (hereafter referred to as Rec_{inter}) and (2) Rec domains that constitute the terminal phosphoryl acceptors (hereafter referred to as Rec_{term}) and typically control the activity of associated effector domains in RRs. Rec-only proteins can belong to either class with e.g., MrrA shuttling phosphoryl groups between various kinases[5] and CpdR regulating the activity of a protease via complex formation[6] (Fig. 1C).

Rec domains of HHKs are of the Rec_{inter} type by definition. It has been estimated that they make up about 10% of all known Rec domains[1], but only very little is known about their structural and functional properties[7,8]. To test for distinguishing features of Rec_{inter} domains, we have analyzed the structure and dynamics of the C-terminal Rec domain of the well-studied HHK CckA ($CckA^{Rec}$). Sequence comparisons of $CckA^{Rec}$ homologs with Rec_{term} homologs revealed subgroup-specific motifs. Unexpectedly, a FATGUY motif, first identified in Rec-only proteins[9,10], is a conserved feature of $CckA^{Rec}$ orthologs.

CckA initiates the *Caulobacter crescentus* CckA - ChpT - CtrA/CpdR phosphorelay (Fig. 1C) which is central to the regulation of the cell cycle *via* the transcription master regulator CtrA[11]. As endogenous input signals, DivL[12,13] and the second messenger c-di-GMP[14], the

concentration of which varies over the cell cycle[15], have been identified. The structure of $CckA^{Rec}$ together with that of the previously determined structure of $CckA^{DHp-CA16}$ allowed us to model the intramolecular phosphotransfer competent conformation of CckA based on the structure of the ChpT/CtrA complex from *B. abortus*[17]. Most interface residues are not conserved but show very clear co-evolution amongst HHK sequences. This probably prevents cross-talk of the Rec domain with downstream HPt partners of the various phosphorelays.

Results

Crystal structure of $CckA^{Rec}$

The crystal structure of the Rec domain of CckA ($CckA^{Rec}$, residues 568 - 691) was determined to very high resolution (1.25 Å resolution) by molecular replacement (Fig. 2A). Data collection and refinement statistics are given in Supplementary Table 1. The structure is defined by continuous electron density from residues 570 to 689 except for residues 654 to 663 (Fig. S1). $CckA^{Rec}$ exhibits the canonical $(\beta/\alpha)_5$ fold of Rec domains with a central five-stranded parallel β-sheet and the β-strands connected by cross-over helices[18] . However, the cross-over segment from β4 to β5 (β4 - β5 linker) is partially disordered and not folded into a canonical α4 helix (Fig. 2A).

The structure of $CckA^{Rec}$ superimposes only moderately well (rmsd = 1.6 Å for 104 Cα positions) with the Rec domain of the CtrA homolog from *B. abortus* (Figs. 2A, B), although both domains are functionally engaged with the histidine phosphotransferase ChpT during phosphorelay (Fig. 1C). Rec structures with a disordered β4 - β5 segment, i.e. a missing α4 helix, have been seen before, e.g., for non-activated PhoB (2iyn) or for the stand-alone Rec domain Q1CZZ7_MYXXD (3nhm). A β4 - β5 segment with an irregular loop structure is seen in the stand-alone Rec protein Mhun_0886 (3cg4, Fig. 2C). The cryptic Rec1 domain of the HHK ShkA involved in c-di-GMP binding shows an irregular β3 - β4 linker (6qrl, Fig. 2D) and, in the Rec1 domain of HHK RcsC (2ayx), three helices are replaced by irregular loops. Thus, the Rec-fold appears stable enough to tolerate such variations in elements that may be functionally dispensable or involved in the specialized function.

As anticipated from its canonical fold, the $CckA^{Rec}$ structure aligns well with many Rec domains in the PDB database including prokaryotic as well as yeast and plant homologs. When ranked according to the PDBeFold Q score, the top hit is a structure of Spo0F from *Bacillus subtilis* (3q15, rmsd = 1.2 Å for 100 of the 109 $CckA^{Rec}$ Cα positions) followed by two other stand-alone Rec proteins, DivK_CAUCR and Q1CZZ7_MYXXD.

The asymmetric unit of the $CckA^{Rec}$ crystals contains one Rec monomer and, since the crystallographic space-group (I2) is devoid of dyad axes, no two-fold dimers are present within the crystal. Indeed, as measured by SEC-MALS, $CckA^{Rec}$ was found to be monomeric in solution up to concentrations of around 1 mM (Fig. S2).

Active site of CckA^{Rec} exhibits activated conformation

Figures 3A,B show a close-up view of the phosphorylation site (D623) with surrounding residues and hydrating water molecules. Unexpectedly, there is no magnesium ion, but the divalent cation binding site is occupied by a water molecule (W37). K673 (from the β5 - α5 loop) implicated in phospho-stabilisation and the “switch” residues S651 (end of β4) and F670 (β5) are well defined by electron density with the latter residue exhibiting two alternative rotamer conformations.

Though the CckA^{Rec} structure has been determined in absence of the phosphoryl-mimic beryllofluoride and shows no bound divalent cation, the active site is clearly in the activated conformation. This can be inferred from e.g. its comparison with the native and BeF_3^- - modified active site structures of PhoB[19] (Figs. S3A,B). Like activated PhoB^{Rec}, CckA^{Rec} shows (1) a closed β3 - α3 loop with main-chain carbonyl 625 (55 in PhoB^{Rec}) in place for Mg^{++} coordination and (2) the side-chain hydroxyl of S651 (T83 in PhoB^{Rec}) in the inward position ready for forming an H-bond with an incoming BeF_3^- - moiety (Figs. 3C,D). We note, that one of the two alternative conformations of the aromatic switch residue F670 coincides with the inward orientation as seen in activated PhoB (Fig. 3D).

Secondary structure and dynamics of native and BeF_3- modified CckA^{Rec} in solution

To investigate the effect of activation on the structure and dynamics of CckA^{Rec}, NMR studies were performed on native and BeF_3^- bound samples. The 2D [^{15}N,^{1}H]-HSQC spectrum of CckA^{Rec} shows well-dispersed signals indicative of a well-folded protein both for the native and the activated sample (Fig. S4). No peak broadening was observed upon activation, arguing for the absence of oligomerization (Supplementary Table 2). Backbone chemical shifts of Cα- and Cβ-atoms were assigned based on standard triple resonance experiments for nearly all residues with the exception of residues forming the acidic pocket (E577, D578, E579) and the phospho-acceptor D623 and the following residues 624 to 628 of the β3 - α4 loop. These unassigned residues most likely experience intermediate exchange leading to significant line broadening and thus are not visible in 2D [^{15}N,^{1}H]-HSQC experiments.

Chemical shifts correlate strongly with local structure, of particular value are Cα and Cβ chemical shifts that depend on the protein secondary structure. The NMR-based secondary structure assignments for native CckA^{Rec} (Fig 4A, top) are fully consistent with the crystal structure (Fig. 4C), with the exception of the segment connecting β4 with β5, which has significant, but low helical propensity (α4). Upon addition of BeF_3^-, the sequence-specific secondary chemical shifts (Fig. 4A, bottom) remain virtually identical, indicating no change in secondary structure (Fig. 4B)

Figure 4D shows the chemical shift perturbation (CSB) values obtained from comparing native and activated CckA^{Rec} spectra. Residues with strong or medium perturbation all cluster

around the phosphorylation site (Fig. 4E) with residues 648 - 658 (β4/begin of β4 - β5 linker) representing the largest continuous stretch.

To further characterize the backbone dynamics of $CckA^{Rec}$, we performed $^{15}N\{^{1}H\}$-NOE experiments that report on ps- to ns-timescale motions (Fig. 4F). Strikingly, the residues in helix α4 show faster motions (lower HetNOEs) compared to the rest of the protein, suggesting that this segment is in a rapid disordered loop <-> helix equilibrium. Thereby, BeF_3^--induced activation shows no significant effect on this mobility (Fig. 4F).

Concluding, the activation does not significantly affect the secondary structure and dynamics of $CckA^{Rec}$, but local perturbations are seen at several places around the phosphorylation site, most prominently at the end of β4 and the following β4 - β5 linker. The latter segment exhibits moderate helical propensity (corresponding to α4 in canonical Rec domains) and the greatest mobility.

Intramolecular phosphotransfer within an HHK: DHp/Rec association

The second step in the CckA - ChpT - CtrA/CpdR phosphorelay, after CckA auto-phosphorylation, Phosphate is the intra-molecular phosphotransfer from H322 to D623 residing on the Dhp and Rec domains, respectively (Figs. 1B, C). With the structures of both CckA domains known (5idj[16] and 6tne, this study), we set out to model the functionally competent domain arrangement based on the crystal structure of the complex between $ChpT^{CA\text{-}DHp}$ and $CtrA^{Rec}$ from *Brucella abortus* (4qpj,[17]). Latter complex is thought to represent a phosphotransfer competent DHp/Rec arrangement. The model was generated by individual superposition of the two CckA domains onto the respective domains of the experimental complex structure using only interface elements (see Methods) without any side-chain adjustments.

Figure 5 shows the side-by-side comparison of the modelled and the template complex. Even without refinement, the CckA phosphotransfer model (Fig. 5A) shows no clashes between main-chain atoms (including Cβ atoms) of the two domains but favourable contacts between residues that are homologous to interacting residues in the experimental structure. Therefore, it can be inferred that, despite low sequence identity, the domain interactions in the two complexes are analogous involving residues of the lower half (towards the helix connector) of the α1'/α2' DHp bundle and the Rec α1 helix (Fig. 5A). Strikingly, only one contact is found strictly conserved when comparing the two interfaces. In CckA, this is formed between A330 and A581 (corresponding to A30 and A11 in ChpT/CtrA) with the short side-chains allowing close contact of the interacting α1 helices (Fig. 5). Other potential contacts involve the conservatively replaced N326/E579 pair (S26/D9 in ChpT/CtrA) and the hydrophobic L333/V585,L589 cluster homologous to the partly polar N33/S15,M19 cluster in ChpT/CtrA. In CckA, an acidic cluster formed by Q337, E350, and E354 may engage in salt-bridges with R588 upon appropriate adjustment of side-chain conformations. In ChpT/CtrA, this is replaced by the apolar L37/L18 contact.

Promiscuous interactions in the CckA - ChpT - CtrA/CpdR phosphorelay

The CckA multistep phosphorelay catalyzes transfer of the phosphoryl group between alternating DHp and Rec domains (Fig. 1C), where the domains positioned centrally in the relay engage sequentially with an acceptor and a donor partner of the same type (e.g., $CckA^{Rec}$ with the DHp domains of CckA and ChpT). The structures of the first three domains of the phosphorelay are now known and the structures of $CtrA^{Rec}$ and CpdR can be determined by homology modeling based on close relatives. Figure 6 shows all structures of the phosphorelay in “open-book” representation to allow easy comparison of the interfaces. Note that the two helices of $CckA^{DHp}$ that are engaged in the interaction belong to separate subunits of the dimeric 4-helix bundle. This is due to the opposite handedness of the helix connector compared to $ChpT^{DHp16,20}$. Nevertheless, the helix pairs of CckA and ChpT (Fig. 6) superimpose rather well with an rmsd of 1.3 Å (43 Cα positions).

The DHp/Rec interface of CckA, as derived in the preceding chapter (Fig. 5A), can be divided into four contact patches with the constituting residues color-coded in Fig. 6. From the top, residues N326/E579 (blue) form a polar interaction, A330/A581 (salmon) allow the close approach of the interacting helices, residues Q337,E350,E354/R588 that may form favorable ionic interactions (yellow), and the apolar L333/V585,L589 contact (green). A contact matrix of these CckA domain interactions, and for the other phosphorelay contacts as well. The alanine - alanine contact (salmon), also observed in the *Brucella* ChpT/CtrA complex, is conserved throughout the relay (except for CpdR, where it is replaced by a serine) and appears crucial for the close contact between the interacting helices. The blue intramolecular CckA contact residues are replaced in the other partners but have kept their polar/acidic property. Two of the three acidic $CckA^{DHp}$ residues potentially interacting with R588 of $CckA^{Rec}$ (yellow) are replaced by apolar residues in $ChpT^{DHp}$, thus extending the apolar green patch. This could be important for $ChpT^{DHp}$ to be able to interact with both the largely apolar patch on $CtrA^{Rec}$ and the mixed basic/apolar patches on $CckA^{Rec}$ and CpdR. To summarize, the patches proposed to mediate the intramolecular DHp/Rec contact in CckA, appear involved in all contacts of the phosphorelay. However, in most cases, the interfacial residues are not strictly conserved but conservatively replaced, although there are also a few more drastic substitutions from ionic to apolar residues.

Two classes of Rec domains in multi-step phosphorelays: Rec_{inter} and Rec_{term}

Multi-step phosphorelays (Fig. 1B) involve at least two types of Rec domains with distinct functional roles: (1) intermediary Rec_{inter} domains, which pass the phosphoryl group from an acceptor to a donor, and (2) terminal Rec_{term} domains at the end of the relay. C-terminal Rec domains of HHKs shuttle the phosphoryl group between DHp domains and can, therefore, be classified as bona-fide Rec_{inter} domains. In contrast, Rec_{term} domains are typically part of

response regulators and allosterically control the activity of a linked effector domain. How the functional differences between the two types of Rec domains are reflected in their sequences and structures is analysed below. For a comparative analysis, Hidden Markov Models (HMM) based on the sequences of $CckA^{Rec}$ and $CtrA^{Rec}$ were created to generate corresponding sequence libraries with sufficient variation to reveal class-specific differences (Fig. 7).

All sequences obey the Rec fold as indicated by the overall conservation (grey background in Fig. 7) of crucial Pro, Gly, or hydrophobic residues (CckA: L574, L590, Y595, P627, G631, A654) and show conservation of the phosphorylatable aspartate (D623) and of the residues involved in phosphoryl-stabilization (K673) or magnesium-binding (E577, D578). For Rec_{term} domains, structural S/T - Y/F coupling has been described as an allosteric mechanism for activation, whereby, upon phosphorylation, the S/T residue is pulled towards the phosphoryl group leading to a change in the Y/F rotamer[18]. In all sequences, an S or T residue (S651 in CckA) is conserved at the end of β4 consistent with its role in phosphoryl-stabilization (see Fig. S3B). However, while a Y residue is observed on β5 in all $CtrA^{Rec}$ orthologs, there is variability at this position (F670) in $CckA^{Rec}$ orthologs, which would be consistent with the loss of allosteric signalling towards the 4-5-5 face in latter group. Finally, the conserved D/E in CckA position 579 seems to contribute to DHp recognition (Figs. 5 and 6) and the aspartate preceding β3 (D618 in CckA) is probably conserved for structural reasons, as its side-chain is engaged in H-bonding with main-chain amide 572. In summary, and not surprisingly, the overall sequence comparison confirms conservation of the Rec fold and the presence of a well-conserved phosphorylation site for both Rec classes.

Comparison of the $CckA^{Rec}$ and $CtrA^{Rec}$ homologs is most relevant to reveal class-specific positions (Fig. 7). Most of the differentially conserved residues play a structural role ($CckA^{Rec}$: G594, A600, A606, V624, M626, P632, P643, F649, V684; $CtrA^{Rec}$: L54, P74, L78, G94), demonstrating evolution of Rec into two distinct folds that are, however, still closely related (rmsd = 1.5 Å / 99 Cα positions and 25% sequence identity between $CckA^{Rec}$ and $CtrA^{Rec}$ of *C. crescentus*).

More interesting are the positions that may indicate functional specialisation. In $CckA^{Rec}$, these are R583 of α1, which is predicted to mediate contact with DHp partners, and the segment 649 - 655 encompassing part of β4 and the start of the β4-β5 linker showing a FxSGY motif. The segment comprises the phosphoryl-coordinating S651 (S/T position) and Y653, which is exposed and, therefore, probably conserved for functional and not structural reasons. Intriguingly, for the Rec-only proteins Sma0014 and SdrG a similar motif has been identified previously[9,10], see Fig. S5B. The motif has been dubbed “FATGUY”[10], a nomenclature we adopt below. This prompted us to generate HMM profiles also for the Rec-only proteins CpdR of the CckA phosphorelay and MrrA, which has recently been shown to constitute a central phosphorylation hub, as it mediates phosphotransfer between various HKs in *C. crescentus*[14]. Intriguingly, also the logos of these proteins (Fig. S5A) reveal a FATGUY motif. An HMM

profile was also generated for the C-terminal Rec domain of the HHK ShkA, another well-studied HHK in *C. crescentus*[21,22]. This profile clearly lacks the FATGUY motif.

In contrast to $CckA^{Rec}$, the $CtrA^{Rec}$ logo clearly shows the hall-marks of OmpR-like Rec domains with conserved ionic residues on β5 and α5 that are known to mediate Rec dimerization upon activation[19]. For $CtrA^{Rec}$, the predicted inter-subunit salt bridges would be D96 - R118, D97 - R111 as indicated in Fig. 7. The remaining residues conserved specifically in $CtrA^{Rec}$ sequences are R67 and R117, whose side-chains are H-bonded to main-chain carbonyls of the same or adjacent subunit, respectively, and E107, which forms an intra-molecular salt-bridge with the aforementioned R111.

The HMM derived logos (Fig. S5A) allow classification of individual Rec sequences as shown in Figs. S5B. The profiles show good orthogonal discrimination between the founder sequences (Fig. S5A, top half), with the exception of some overlap between $CckA^{Rec}$ and CpdR. The lower half of Fig. S5B shows the classification of some selected, structurally well-characterized Rec proteins. Sma0114[10] and SdrG[23] clearly fit the MrrA profile, whereas all HHKs with known C-terminal Rec structure match the $ShkA^{Rec}$ profile and are, therefore, not representatives for the $CckA^{Rec}$ group.

The conservation properties have been mapped onto the Rec surfaces to demonstrate the similarities and differences of the two classes (Fig. 8). Both classes show a canonical phosphorylation site including an acidic pocket for magnesium binding. Otherwise, surface conservation is completely different between the two classes (indicated in orange and green in Fig. 8). In $CckA^{Rec}$, a conserved surface patch is formed by residues of the FATGUY motif from β4 / β4-β5 and residues V624, P632. Latter residues, however, may be covered by the flexible β4 - β5 linker. Furthermore, there is residue R583, which is part of an intramolecular salt-bridge in $CckA^{Rec}$ and R588, which is most likely involved in DHp recognition (Fig. 5A). In $CtrA^{Rec}$, β5 and α5 residues form an extended conserved patch that is involved in dimerization upon activation (see also Fig. S3C).

Co-variation between DHp and Rec residues in HHKs

Despite playing a central role in phosphotransfer, the surface of Rec α1, which engages with cognate DHp domains, is remarkably variable amongst homologs (Fig. 7). This has been attributed to the need to prevent cross-talk between the individual phosphorelays in a given organism[24]. Apparently, cognate contacts can diversify in the course of evolution through co-variation of interacting residues. For two-component systems, this has been demonstrated impressively by Laub and coworkers in their pioneering work more than 10 years ago[25] in which they selected cognate HK and RR pairs based on experimental data or genetic organization (syntheny) to study DHp/Rec covariation. For the study of DHp/Rec recognition in HHKs, the cognate pairs are obviously already defined, because they are part of the same

polypeptide chain. Since, furthermore, the sequence data base has increased considerably over the last decade, a study on co-variation in HHKs seemed promising.

The EVfold analysis of more than 8000 HHK DHp-CA-Rec sequences (Fig. S6) shows, as expected, strong co-variation of residues forming intra-domain contacts, but also between DHp-α1',α2' and Rec-α1 residues. A zoom into the EVfold matrix (Fig. 9A) shows that the hits correlate very well with the DHp/Rec contacts as calculated from the CckA phosphotransfer model (Fig. 5A). Noteworthy, four co-varying pairs (labeled in bold red in Fig. 9A) can be predicted to form salt-bridges in HHKs as deduced from their substitution matrices shown in Fig. 9B. In all four cases, salt-bridges are also observed in the charge reversed configuration (e.g. R/E or E/R are observed about equally often for the pair 341/592), providing further evidence for interaction between these residues in HHKs. Note that, in CckA, only one of these pairs, E350/R588, constitutes an ion pair. To summarize, the straightforward HHK co-variation analysis gave strong, independent evidence for the validity of the proposed phosphotransfer competent DHp/Rec arrangement. Further studies may exploit the rich information in the substitution matrices of the co-varying residues to understand better how the variation of interface residue types allows specific recognition between cognate domains while preventing cross-talk between phosphorelays.

Discussion

Degenerated $CckA^{Rec}$ fold

Rec domains of RRs constitute the terminal phosphoryl-acceptors of TCSs. Such Rec_{term} domains have been studied intensively over several decades and hundreds of structures are known, both in the native and the activated form[1]. Typically, upon activation, a conserved S/T residue is pulled towards the phospho-aspartate accompanied by allosteric changes involving the β4 - α4 loop and the α4 helix. In addition, a conserved Tyr/Phe rotates inwards to stabilize the active conformation[18,26]. Depending on the particular RR, these changes can then induce a plethora of distinct effects as there is dimerization (OmpR), oligomerization (NtrC), change in dimeric structure (DgcR), relief of effector domain obstruction (CheB), or change in the binding site for a downstream partner (CheY).

Rec domains of HHKs are intermediaries in phosphorelays in that they shuttle the phosphoryl group between two DHp (or Hpt) partners. As an Rec_{inter} prototype, we have chosen the C-terminal Rec domain of the well-studied HHK CckA from *C. crescentus*[14,16]. $CckA^{Rec}$ obeys the canonical Rec fold, but with a comparatively low helix propensity and missing electron density for the β4 - β5 linker as derived from NMR and X-ray analysis. In canonical Rec domains, this segment is typically folded to a well-defined helix α4. However, a recent comprehensive NMR and modeling study on NtrC[27] suggests that only in the activated state helix α4 is well defined and in fact of maximal length. In contrast, the secondary structure

of $CckA^{Rec}$ remained unaltered upon activation by BeF_3- suggesting that the β4 - β5 linker is not subject to allosteric alteration.

Missing α-helices have been reported for other Rec domains (see e.g. Fig. 2), but to our knowledge only for Rec-only proteins (e.g. Sma0114 and SdrG, see further below) or accessory (phosphorylation-incompetent) Rec-like domains of HHKs (RcsC[28] and ShkA[22]). Thus, the Rec-fold appears to be a stable framework tolerating the loss of helices and such variation may indicate neutral evolution or functional specialization. For CckA, the latter reason can probably be excluded, since the β4 - β5 linker (with the exception of the first few residues) is highly variable and not in a position to interact with phosphotransfer partners (see e.g. the Spo0B/Spo0F and ChpT/$CtrA^{Rec}$ complex structures[29,17].

Preformed $CckA^{Rec}$ active site

Unusual for Rec domains, unmodified $CckA^{Rec}$ shows the active site in the activated conformation with the β3 - α3 loop closed down and the conserved S651 at the end of β4 in a position to coordinate a phosphoryl group bound to the active aspartate (Figs. 3C, S3). Although a preformed active site has also been reported for unmodified PhoP, in this case activation was apparently triggered by allosteric coupling with the homo-dimer interface[30]. In contrast, $CckA^{Rec}$ is monomeric in the crystal lattice as it is in solution. With a fully preformed active site, no significant structural changes would be expected upon phosphorylation or BeF_3-modification, consistent with the NMR chemical shift perturbation analysis (Fig. 4). In summary, unlike the well-known phosphorylation-induced structural changes in Rec_{term} domains, there is no evidence that changes of similar magnitude take place in $CckA^{Rec}$ and the same would be expected for its orthologs.

Phosphotransfer complex model and promiscuity of HHK Recs

The intramolecular CckA DHp/Rec association has been modeled based on a known phosphotransfer complex (ChpT/CtrA^{Rec} complex from B. abortus {Willet}). It has to be noted that, in the modelled complex, the His - Asp distance is too long for associative phosphotransfer (10.4 Å compared to 5.9 Å in ChpT/CtrA^{Rec}). The difference in the histidine position appears to be due to a distinct orientation of the N-terminal end of CckA α1' preceding a smooth bend around residue 328 (in ChpT, there is a sharp kink due to the presence of a proline in position 27 corresponding to CckA residue 327). It is well conceivable that a tertiary change in the DHp domain of CckA, i.e. change in α1' bending, can be induced by Rec/CA interactions. Such interactions have not been considered here and are not evident in the covariation analysis (Fig. S6), but could move the histidine into the position required for phosphotransfer. In the ChpT/CtrA^{Rec} complex, residues of the Rec β4 - α4 loop interact with the CA-domain[17]. In CckA, such interactions could involve the Y of the FATGUY motif and subsequent residues from the Rec β4 - β5 linker and may contribute to affinity, but also to α1' bending for efficient phosphotransfer.

Multi-step phosphorelays involve at least two domains that act as intermediaries (e.g. the two central domains of a His-Asp-His-Asp phosphorelay) and interact successively with two partners of the same fold. We have shown that the involved interfaces show surprisingly little conservation (Fig. 6) suggesting that the partners are evolutionary not particularly close. Apparently, based on the same frameworks, there are various solutions to form catalytically competent domain associations by residue-type variation. This has been demonstrated already very convincingly by co-variation analysis of cognate HK/RR pairs[25] and has been associated with the need to insulate the various TCSs of a given organism against mutual interference. Our HHK analysis (Fig. 9A) shows very clear intra-domain covariation, probably due to the large number of sequences considered, and is broadly consistent with the previous HK/RR results[25] and the phosphotransfer model (Fig. 5A). Individual substitution matrices (Fig. 9B) demonstrate the extensive repertoire of residue combinations for selected pairs, including charge reversal of salt bridges.

Lower specificity of the intramolecular recognition in HHKs compared to cognate HK/RR pairs has been reported and attributed to the relaxed constraints for phosphotransfer due to the high local concentration of the covalently attached Rec domain[31,32]. Here, by being able to analyze a vast number of sequences, we have found very significant covariation between DHp and Rec domains of HHKs. It would be interesting to see, whether covariation between cognate DHp/Rec from separate proteins turns out to be even more pronounced, when using a similarly large database. In any case, it should be considered that an HHK Rec domain not only has to recognize its covalently attached DHp domain, but also its specific downstream HPt partner, with latter interaction subject to the same evolutionary constraints as in canonical HK/RR systems.

Rec classification

Most Rec domains can be identified easily by the match of their sequences with the pfam motif pf00072, which covers the active site and residues crucial for the $(\beta\alpha)_5$ sandwich fold. A very useful sub-classification of Rec domains has been performed on the basis of their domain context by Galperin (https://www.ncbi.nlm.nih.gov/Complete_Genomes/RRcensus.html[2]. However, it has not yet been investigated whether there are intrinsic Rec features that correlate with this sub-classification. In the Conserved Domain Database of the NCBI, a very finely graded Rec sub-classification of the Rec entry (cd00156) with 82 “models” based on sequence similarity can be found (https://www.ncbi.nlm.nih.gov/Structure/cdd/cdd.shtml)[33]. However, many of the subgroups consist of only a few closely related sequences.

For our comparative Rec sequence analysis (Fig. 7), the chosen threshold for sequence selection resulted in a moderate mean pairwise identity of about 45 % within the subgroups. Such sequence variability made it possible to uncover subgroup specific motifs and to derive well discriminating HMM profiles. Indeed, searching with the $CckA^{Rec}$ profile against the Reference Proteome database (as implemented in HMMER) using an E-threshold of $1e\text{-}^{25}$ retrieved HHKs and Rec-only proteins exclusively. Conversely, when searching with the $CtrA^{Rec}$ profile, as expected RRs were found, but also HKs with N-terminal, but not C-terminal, Rec domains domains were found.

As expected, the $CtrA^{Rec}$ profile is specific only for the OmpR-Rec class and not for Rec_{term} domains in general. While probably all Rec_{term} domains have an inbuild allosteric mechanism to control their output domain function, the details appear to be diverse. Since part of the $CtrA^{Rec}$ profile comprises residues that allow OmpR-Rec domains to homo-dimerize via the 4-5-5 face, Rec_{term} domains with other allosteric mechanisms (NtrC, CheY, etc.) will not be recognized by the $CtrA^{Rec}$ profile.

Similarly, not all Rec_{inter} domains conform to the $CckA^{Rec}$ profile. In fact, the C-terminal Rec domains of most *C. crescentus* HHKs show similarity to the corresponding domain of ShkA and not of CckA. It would be interesting to learn more about the phosphotransfer mechanism of $ShkA^{Rec}$ domains. In particular, their resemblance to $CtrA^{Rec}$ (i.e. OmpR-type Rec domains) is intriguing. Thus, as with the Rec_{term} domains, the Rec domains that act as intermediaries in phosphotransfer are not a monophyletic group.

Rec-only proteins and FATGUY motif

Rec-only proteins form a large group with diverse functions. A prominent group is the chemotactic CheY proteins that regulate bacterial motility. CheY phosphorylation affects the affinity of e.g. FliM motor peptides due to an allosteric change of the binding site at the 4- 5-5 face accompanied by Y-T coupling similar as in transcriptional RRs. The Rec-only protein CpdR of the branched CckA phosphorelay is required to enable ClpXP mediated CtrA

degradation[6] . Thereby, CpdR seems not to act as a classical adaptor for CtrA degradation (e.g. SspB for SspA tagged proteins[34], but rather prime the proteolytic complex for this activity. Since CpdR phosphorylation interferes with the priming function, both branches of the CckA phosphorelay work together to ensure tight transcriptional regulation (Fig. 1C). It has been shown that CpdR interacts with the N-terminal Zn-finger domain of ClpX[35], but only in its non-phosphorylated state. No details about the binding mode are known and whether phosphorylation interferes directly or allosterically with binding, though residues on α5 seem involved in the interaction arguing for an allosteric effect[35].

The sequence logo of CpdR does not reveal additionally conserved residues that could potentially interact with ClpX (Fig. S5A, compare with the $CtrA^{Rec}$ logo with its conserved residues at the C-terminus mediating homo-dimerization). Either such residues are co-varying with ClpX or residues of the CpdR active site are mediating the contact with ClpX, which would also explain the dependence of binding on the CpdR phosphorylation state. Strikingly, CpdR reveals a FATGUY-like motif at β4 and the following loop as seen in $CckA^{Rec}$. Given that both domains have to engage with ChpT for phosphotransfer, it is likely that the motif is related to this specific function, especially since the overall sequence similarity of the two domains is only moderate (35 %).

A role of the FATGUY motif in phosphotransfer between Rec and DHp or Hpt domains would be consistent with the occurrence of the motif in other, well-studied proteins that act as Rec-only intermediaries: the phosphorylation hub MrrA[5], SdrG[10,36] from the general stress response and Sma0114[23]. Latter two proteins have been studied by NMR in their native and activated form. For Sma0114, it was initially proposed that the FATGUY motif would indicate an alternative mechanism to Y-T coupling, considering a missing α4 helix and a missing aromatic residue on β5[9]. Such a mechanism, however, was refuted by the subsequent investigation into structure and dynamics of the activated form of Sma0114 that showed only minor changes in the motif[23]. For SdrG, a change in the orientation of T83 and a repacking of a (not conserved) phenylalanine from the β4 - β5 linker (F94) with the hydrophobic core upon activation has been reported[10]. However, the considerable variation in the ensemble of the activated structures makes a detailed description of activation-induced changes difficult. We note that all aforementioned NMR structures were modeled with a trans-peptide bond between lysine 105 and the following proline, although a cis-peptide bond between these two conserved residues is a hallmark of the Rec-fold[18] and is required to place the conserved lysine in the active site (Figs. 3C, D). Thus, the proposed role of the lysine to switch from an outward to an inward orientation in signaling has to be questioned.

In summary, the significance of the FATGUY is still not resolved. It is present in Rec_{inter} domains (such as $CckA^{Rec}$, MrrA, Sma0114, and SdrG), which most likely do not rely on an allosteric control of the 4-5-5 face for their phosphotransfer function. The same may be true for CpdR, though positioned at the end of the phosphorelay. Sterically, it appears possible

that residues from the end of the motif (in particular the tyrosine) interact with the CA domains of their phosphotransfer partners to enhance affinity, but perhaps also to control DHp conformation allosterically.

Based on the current study, we suggest that intermediary Rec domains play a rather passive role in phosphotransfer. Phosphorylation of their preconfigured active site will not induce structural changes such as the inward movement of the S/T residue and concomitant allosteric changes in Rec_{term} domains evolved to control output domain function or partner recognition. Here we have analyzed $CckA^{Rec}$ and its orthologs. Future structure/function studies on other Rec_{inter} families will show whether these findings can be generalized and will allow further sub-classification of Rec domains to allow comprehensive sequence-based assignment of Rec function (Rec_{inter} versus Rec_{term}) in multi-step phosphorelays.

Material and Methods

Cloning and protein expression

The DNA fragments corresponding to the receiver (Rec) domain (568-691) of wild-type CckA (Uniprot: Q9X688) was amplified first by PCR using the primers pairs, Forward: Q5SDM_CckARec_F; Reverse: Q5SDM_CckARec_R. To add a N-terminal His-tag, a second PCR was applied on the first PCR product by using the primers pairs, Forward: Q5SDM_CckARec_N-histag_F; Reverse: Q5SDM_CckARec_N-histag_R (Supplementary table 3). The second PCR product corresponding to 6-His_CckA-Rec was treated with DpnI to eliminate template plasmids and cloned using ligation-independent cloning {Aslandis et al., 1990} into pET28a vector (Novagen) yielding pET28-CckA-Rec plasmid. After successful cloning, plic06-CckA-Rec plasmids were extracted from E. coli DH5α cells following QIAprep Spin Miniprep Kit protocol (QIAGEN) and used to transform the expression strains E. coli BL21(DE3) or similarly efficient Rosetta cells (Novagen). For protein expression, adequate amounts of LB-Kan media were inoculated with 1% pre-culture of transformed cells. Cultures were grown at an incubation temperature of 37 °C and induced with 1 mM isopropyl 1-thio-β-D-galactopyranoside (IPTG) upon reaching an OD600 of 0.6 – 0.8. The incubation temperature was reduced to 21 °C for overnight protein expression. Cells were harvested by centrifugation at 9’000 RCF for 10 minutes at 4 °C. Pellets were stored at -20 °C or lysed immediately.

Protein purification

Purification was entirely performed at 4 °C. Pellets were homogenized in lysis buffer containing immobilized metal affinity chromatography (IMAC) loading buffer (500 mM NaCl, 30 mM Tris-HCl, 5 mM MgCl2, 20 mM Imidazole, pH 7.5), complete EDTA-free protease inhibitors (Roche) and bovine pancreas DNase I (Roche). Cell lysis was performed using

French-press (3 passes, 10'000 psi). The lysate was ultracentrifuged at 31,000 RCF for 1 hour (Thermo Fisher Scientific centrifuge), to remove cell debris and suspended particles. The clear supernatant was applied on a 5 mL Ni-NTA column (GE Healthcare) pre-equilibrated with IMAC loading buffer. Bound protein was eluted with a linear gradient of IMAC elution buffer (500 mM NaCl, 30 mM Tris-HCl, 5 mM MgCl2, 500 mM Imidazole, pH 7.5) using an ÄKTA Purifier system (GE Healthcare). Fractions containing the desired protein were pooled and concentrated to a volume of 5 mL. The concentrated protein was centrifuged at 16,000 x g at 4°C for 15 min and loaded onto a Superdex 75 gel filtration column (Amersham Biosciences) equilibrated with 30 mM Tris/HCl pH 7.5, 5 mM $MgCl_2$, 100 mM NaCl, 1mM DTT. The concentrations of the collected samples were quantified by UV absorption with a NanoDrop 2000 spectrophotometer (Thermo Fisher Scientific) and either used freshly (e.g. for crystallization) or stored at -80 °C.

Crystallization

Protein solubilised in SEC buffer (see above) was crystallised using the sitting-drop vapor diffusion method. Sets of 3-drop MRC plates were prepared with a Gryphon robot (Art Robbins Instruments). $CckA^{Rec}$ was crystallised at three concentrations 20 mg/ml, 10 mg/mL, 5 mg/mL, with a crystallization mixture consisting of 0.15 M KSCN, 0.1 M Na Cacod 6.5 pH, 20 % v/v PEG 600 (Clear Strategy II-D5) at room temperature.

Data collection and structure determination

All single crystal X-ray diffraction data sets were collected at PXI beam line of Swiss Light source, Villigen, Switzerland.) at 100 K. Diffraction data sets were processed either with iMOSFLM[37] or XDS[38], and the resulting intensities were scaled using SCALA from CCP4/CCP4i2 suite[39] . The crystal structure of $CckA^{Rec}$ was solved by molecular replacement using native structure of DgcR (PDB code, 6ZXM) as a search model using Molrep[40]. Further refinement of structures was carried out using REFMAC5 and phenix refinement[41]. Model building was performed using COOT[42] and model validation was carried out with molprobity[43]. Crystallographic data processing and refinement statistics are provided in Supplementary Table1.

Solution NMR spectroscopy

Protein samples were prepared in 30 mM MES buffer at pH 6.8 with 100 mM NaCl and 5 mM $MgCl_2$ in 5%/95% D_2O/H_2O with a protein concentration of 0.8 mM. All NMR spectra were recorded at 25 °C on a 700 MHz Bruker Avance spectrometer equipped with a cryogenic triple-resonance probe. For the sequence-specific backbone resonance assignment of [*U*-^{15}N,^{13}C]-labeled $CckA_{Rec}$ with and without bound BeF_3^-, the following NMR experiments were recorded: 2D [^{15}N,^{1}H]-HSQC, 3D HNCACB and 3D CBCA(CO)NH. Chemical shift differences of amide

moieties were calculated as $\Delta\Delta(HN) = ((\delta(^1H_{ref}) - \delta(^1H))^2 + ((\delta(^{15}N_{ref}) - \delta(^{15}N))/5)^2)^{1/2}$. For the characterization of backbone dynamics of [*U*-^{15}N,^{13}C]-labeled CckA^{Rec} with and without bound BeF_3^-, ^{15}N{^{1}H}-NOE experiments were measured. Data were processed using Prosa[46] and analyzed with CARA (Keller R. 2004). The backbone assignment was done manually using CARA. Combined secondary chemical shifts of $^{13}C^{\alpha}$ and $^{13}C^{\beta}$ were calculated relative to the random-coil values of Kjaergaard and Poulson[47]. A 1-2-1 smoothing function was applied to the raw data for the display in Fig. 4A. For the analysis of NMR line widths to infer on the oligomerization state, from the 2D [^{15}N,^{1}H]-HSQC spectra of inactive and activated CckA$_{Rec}$ 1D slices of the F1 (^{15}N) – dimension were extracted that contained the respective residues to be analyzed. The 1D amide proton signal was fitted using a gaussian function and the line width at half maximal intensity was calculated using Topspin 4.0.

SEC-MALS

SEC-MALS measurements for CckA^{Rec} were performed at a sample loading concentration of 13.8 mg/ml; 6.9 mg/ml and 3.5 mg/ml at 25 C in sample buffer using a GE Healthcare Superdex 200 10/300 Increase column on an Agilent 1260 HPLC. Elution was monitored using an Agilent multi-wavelength absorbance detector (data collected at 280 and 254 nm), a Wyatt Heleos II 8+ multi-angle light scattering detector and a Wyatt Optilab rEX differential refractive index detector. The column was equilibrated overnight in the running buffer to obtain stable baseline signals from the detectors before data collection. Inter-detector delay volumes, band broadening corrections, and light-scattering detector normalization were calibrated using an injection of 2 mg/ml BSA solution (ThermoPierce) and standard protocols in ASTRA 6. Weight-averaged molar mass (Mw), elution concentration, and mass distributions of the samples were calculated using the ASTRA 6 software (Wyatt Technology).

Modelling of the phosphotransfer competent CckA DHp/Rec complex

The model of the CckA DHp/Rec complex was generated by (1) superposition of the CckA^{DHp_CA} monomer structure (5idj) onto the A-chain of ChpT from the ChpT/CtrA^{Rec} structure (4qpj) using only the Cα positions of the C-terminal half of α1' and the N-terminal half of α2' of the DHp domains. These elements are part of the interface in the ChpT/CtrARec structure. (2) superposition of CckA_Rec (6tne) onto CtrARec (C-chain of 4qpj) using only the Cα positions of the Rec α1 helices, since this helix is part of the interface in the experimental complex. (3) reassembly of the individually superimposed domain structures into a single file.

Bioinformatics

Sequence logos of Rec domains (Fig. S5A) were calculated from the alignment of homologous sequences obtained by successive phmmer and hmmsearch calculations (using HMMER from the EBI website https://www.ebi.ac.uk/Tools/hmmer/,44) against the Reference Proteomes data base starting with the respective sequences of the C.crescentus homologs

using E thresholds between 1E-20 and 1E-25 depending on the group. In the case of CckARec, only full-length sequences were selected that had the three essential HHK domains (HISKA, HATPase_c, Response_reg) but no additional domains annotated. For CpdR and MrrA, single domain proteins with Response_reg annotation were selected. HMM profile were generated using hmmbuild and were run against selected sequences (Fig. S5B) using hmmscan from a local hmmer (version 3.1) installation. Co-variation in HHK sequences was analyzed by the EV fold webservice https://v2.evcouplings.org/45. Details are given in the respective figure legends.

Figures

Figures were prepared with Pymol (https://pymol.org) and Dino (https://dino3d.org).

Protein Data Bank atomic coordinates

Coordinates and crystal structure factors of $CckA^{Rec}$ have been deposited in the Protein Data Bank (PDB) under the accession number 6TNE.

Author contributions

M.B. performed purifications, crystallization, and biophysical experiments under supervision of B.N.D. B.N.D. and M.B. processed x-ray data, determined structure, built and validated the model. T.S. and M.B. performed bioinformatics analysis. R.B. performed NMR experiments. R.B. and S.H analysed NMR data. B.N.D, M.B and T.S. wrote the manuscript with input from all authors. B.N.D. and T.S. conceived and directed the project.

Acknowledgments

We thank the beamline staff at the Swiss Light Source in Villigen for expert help in data acquisition and T. Sharpe from the Biophysics facility at the Biozentrum Basel for expert biophysical support. We would like to thanks to Firas Fadel for his expert help in cloning.

Competing Interests statement

The authors declare no competing financial interests.

References

1. Gao, R., Bouillet, S. & Stock, A. M. Structural Basis of Response Regulator Function. *Annu Rev Microbiol* 73, 175–197 (2019).

2. Galperin, M. Y. Diversity of structure and function of response regulator output domains. *Curr Opin Microbiol* 13, 150–159 (2010).

3. Teixeira, R. D., Holzschuh, F. & Schirmer, T. Activation mechanism of a small prototypic Rec-GGDEF diguanylate cyclase. *Nat Commun* 12, 2162 (2021).

4. Appleby, J. L., Parkinson, J. S. & Bourret, R. B. Signal transduction via the multi-step phosphorelay: not necessarily a road less traveled. *Cell* 86, 845–848 (1996).

5. Lori, C., Kaczmarczyk, A., Jong, I. de & Jenal, U. A Single-Domain Response Regulator Functions as an Integrating Hub To Coordinate General Stress Response and Development in Alphaproteobacteria. *Mbio* 9, e00809-18 (2018).

6. Iniesta, A. A., McGrath, P. T., Reisenauer, A., McAdams, H. H. & Shapiro, L. A phospho-signaling pathway controls the localization and activity of a protease complex critical for bacterial cell cycle progression. *Proc National Acad Sci* 103, 10935–10940 (2006).

7. Otrusinová, O. *et al.* Conformational dynamics are a key factor in signaling mediated by the receiver domain of a sensor histidine kinase from Arabidopsis thaliana. *J Biol Chem* 292, 17525–17540 (2017).

8. Chen, S. K. *et al.* Structural insights into the histidine-containing phosphotransfer protein and receiver domain of sensor histidine kinase suggest a complex model in the two-component regulatory system in Pseudomonas aeruginosa. *Iucrj* 7, 1–15 (2020).

9. Sheftic, S. R. *et al.* Nuclear magnetic resonance structure and dynamics of the response regulator Sma0114 from Sinorhizobium meliloti. *Biochemistry-us* 51, 6932–6941 (2012).

10. Campagne, S. *et al.* Role of the PFXFATG[G/Y] Motif in the Activation of SdrG, a Response Regulator Involved in the Alphaproteobacterial General Stress Response. *Structure* 24, 1237–1247 (2016).

11. Biondi, E. G. *et al.* Regulation of the bacterial cell cycle by an integrated genetic circuit. *Nature* 444, 899–904 (2006).

12. Blair, J. A. *et al.* Branched signal wiring of an essential bacterial cell-cycle phosphotransfer protein. *Structure* 21, 1590–1601 (2013).

13. Childers, W. S. *et al.* Cell fate regulation governed by a repurposed bacterial histidine kinase. *Plos Biol* 12, e1001979 (2014).

14. Lori, C. *et al.* Cyclic di-GMP acts as a cell cycle oscillator to drive chromosome replication. *Nature* 523, 236–239 (2015).

15. Abel, S. *et al.* Bi-modal distribution of the second messenger c-di-GMP controls cell fate and asymmetry during the caulobacter cell cycle. *Plos Genet* 9, e1003744 (2013).

16. Dubey, B. N. *et al.* Cyclic di-GMP mediates a histidine kinase/phosphatase switch by noncovalent domain cross-linking. *Sci Adv* 2, e1600823-10 (2016).

17. Willett, J. W., Herrou, J., Briegel, A., Rotskoff, G. & Crosson, S. Structural asymmetry in a conserved signaling system that regulates division, replication, and virulence of an intracellular pathogen. *Proc National Acad Sci* 112, E3709-18 (2015).

18. Bourret, R. B. Receiver domain structure and function in response regulator proteins. *Curr Opin Microbiol* 13, 142–149 (2010).

19. Bachhawat, P., Swapna, G. V. T., Montelione, G. T. & Stock, A. M. Mechanism of activation for transcription factor PhoB suggested by different modes of dimerization in the inactive and active states. *Structure* 13, 1353–1363 (2005).

20. Ashenberg, O., Keating, A. E. & Laub, M. T. Helix Bundle Loops Determine Whether Histidine Kinases Autophosphorylate in cis or in trans. *J Mol Biol* 425, 1198–1209 (2013).

21. Kaczmarczyk, A. *et al.* Precise timing of transcription by c-di-GMP coordinates cell cycle and morphogenesis in Caulobacter. *Nat Commun* 11, 816 (2020).

22. Dubey, B. N. *et al.* Hybrid histidine kinase activation by cyclic di-GMP-mediated domain liberation. *P Natl Acad Sci Usa* 117, 1000–1008 (2020).

23. Sheftic, S. R., White, E., Gage, D. J. & Alexandrescu, A. T. NMR structure of the HWE kinase associated response regulator Sma0114 in its activated state. *Biochemistry-us* 53, 311–322 (2014).

24. Capra, E. J. *et al.* Systematic dissection and trajectory-scanning mutagenesis of the molecular interface that ensures specificity of two-component signaling pathways. *Plos Genet* 6, e1001220 (2010).

25. Skerker, J. M. *et al.* Rewiring the specificity of two-component signal transduction systems. *Cell* 133, 1043–1054 (2008).

26. Villali, J., Pontiggia, F., Clarkson, M. W., Hagan, M. F. & Kern, D. Evidence against the "Y-T coupling" mechanism of activation in the response regulator NtrC. *J Mol Biol* 426, 1554–1567 (2014).

27. Pontiggia, F. *et al.* Free energy landscape of activation in a signalling protein at atomic resolution. *Nat Commun* 6, 7284–14 (2015).

28. Rogov, V. V. *et al.* A new structural domain in the Escherichia coli RcsC hybrid sensor kinase connects histidine kinase and phosphoreceiver domains. *J Mol Biol* 364, 68–79 (2006).

29. Varughese, K. I., Tsigelny, I. & Zhao, H. The crystal structure of beryllofluoride Spo0F in complex with the phosphotransferase Spo0B represents a phosphotransfer pretransition state. *J Bacteriol* 188, 4970–4977 (2006).

30. Bachhawat, P. & Stock, A. M. Crystal structures of the receiver domain of the response regulator PhoP from Escherichia coli in the absence and presence of the phosphoryl analog beryllofluoride. *J Bacteriol* 189, 5987–95 (2007).

31. Capra, E. J. *et al.* Spatial tethering of kinases to their substrates relaxes evolutionary constraints on specificity. *Mol Microbiol* 86, 1393–1403 (2012).

32. Capra, E. J. & Laub, M. T. Evolution of two-component signal transduction systems. *Annu Rev Microbiol* 66, 325–347 (2012).

33. Lu, S. *et al.* CDD/SPARCLE: the conserved domain database in 2020. *Nucleic Acids Res* 48, D265–D268 (2020).

34. Bolon, D. N., Wah, D. A., Hersch, G. L., Baker, T. A. & Sauer, R. T. Bivalent tethering of SspB to ClpXP is required for efficient substrate delivery: a protein-design study. *Mol Cell* 13, 443–449 (2004).

35. Lau, J., Hernandez-Alicea, L., Vass, R. H. & Chien, P. A Phosphosignaling Adaptor Primes the AAA+ Protease ClpXP to Drive Cell Cycle-Regulated Proteolysis. *Mol Cell* 59, 104–116 (2015).

36. Gottschlich, L., Bortfeld-Miller, M., Gäbelein, C., Dintner, S. & Vorholt, J. A. Phosphorelay through the bifunctional phosphotransferase PhyT controls the general stress response in an alphaproteobacterium. *Plos Genet* 14, e1007294 (2018).

37. Leslie, A. G. W. The integration of macromolecular diffraction data. *Acta Crystallogr Sect D Biological Crystallogr* 62, (2006).

38. Kabsch, W. XDS. *Acta Crystallogr Sect D Biological Crystallogr* 66, (2010).

39. Potterton, L. *et al.* CCP4i2: the new graphical user interface to the CCP4 program suite. *Acta Crystallogr Sect D Struct Biology* 74, 68–84 (2018).

40. Vagin, A. & Teplyakov, A. Molecular replacement with MOLREP. *Acta Crystallogr Sect D Biological Crystallogr* 66, 22–25 (2010).

41. Terwilliger, T. C. *et al.* Iterative model building, structure refinement and density modification with the PHENIX AutoBuild wizard. *Acta Crystallogr Sect D Biological Crystallogr* 64, 61–69 (2008).

42. Emsley, P. & Cowtan, K. Coot: model-building tools for molecular graphics. *Acta Crystallogr Sect D Biological Crystallogr* 60, 2126–2132 (2004).

43. Williams, C. J. *et al.* MolProbity: More and better reference data for improved all-atom structure validation. *Protein Sci* 27, 293–315 (2018).

44. Potter, S. C. *et al.* HMMER web server: 2018 update. *Nucleic Acids Res* 46, W200–W204 (2018).

45. Marks, D. S. et al. Protein 3D structure computed from evolutionary sequence variation. Plos One 6, e28766 (2011).

46. Güntert, P., Dötsch, V., Wider, G. & Wüthrich, K. Processing of multi-dimensional NMR data with the new software PROSA. J Biomol Nmr 2, 619–629 (1992).

47. Kjaergaard, M., Brander, S. & Poulsen, F. M. Random coil chemical shift for intrinsically disordered proteins: effects of temperature and pH. J Biomol Nmr 49, 139–49 (2011).

Figures and Table

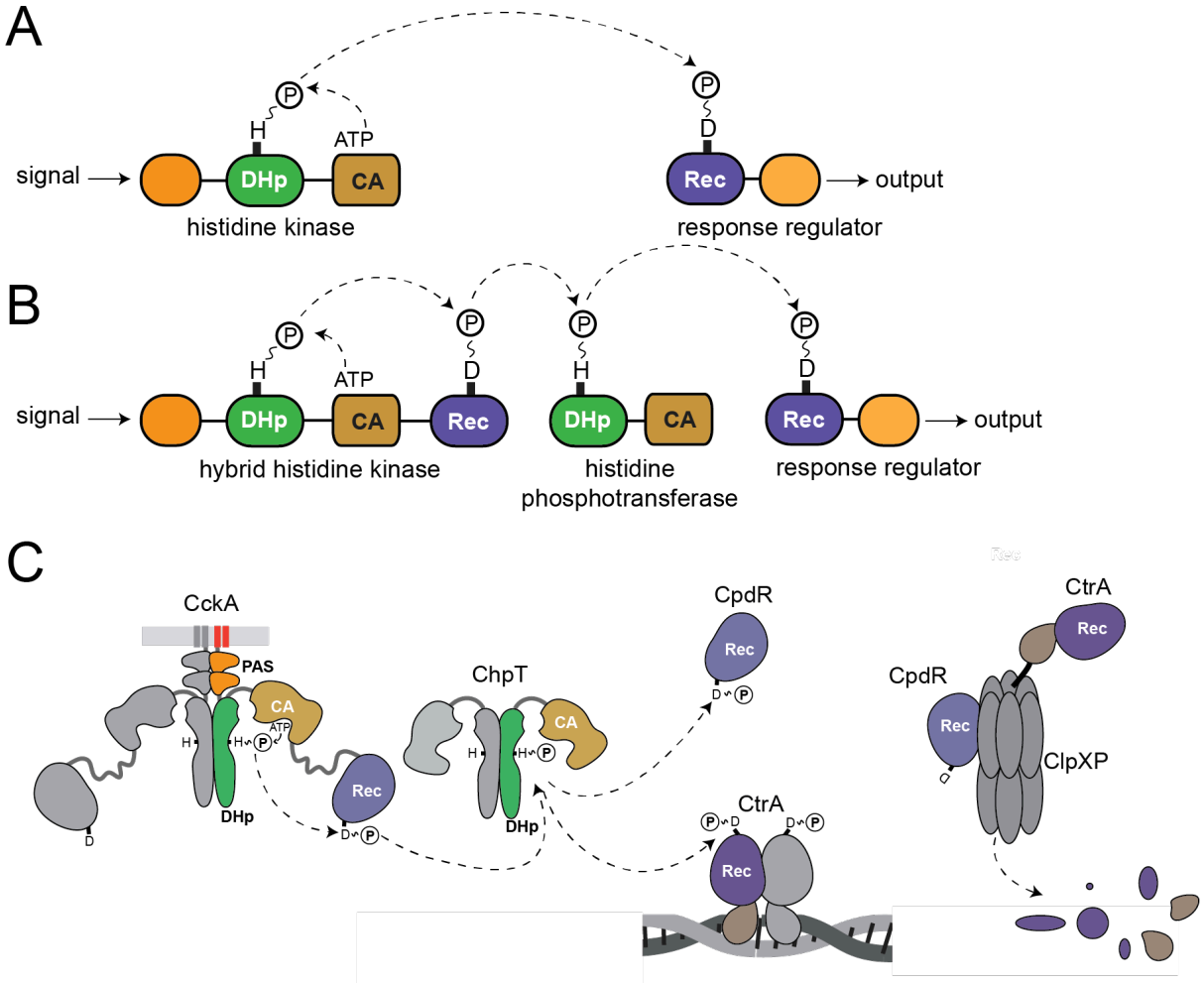

Figure 1. Schematic representation of two-component vs multi-component signalling pathways and the CckA - ChpT - CtrA/CpdR phosphorelay system.
(A) Classical two-component system comprised of a histidine kinase and a response regulator. Domain organisation and residues involved in phosphoryl transfer are indicated.
(B) Multistep phosphorelay consisting of a hybrid histidine kinase (HHK), a histidine phosphotransferase, and a response regulator.
(C) CckA–ChpT–CtrA/CpdR phosphorelay of *Caulobacter crescentus*. Each subunit of homo-dimeric HHK CckA (left) is comprised of two transmembrane helices (red), two Per-Arnt-Sim (PAS) domains (orange), a dimerization/histidine phosphotransfer (DHp, green) domain, a catalytic ATP binding (CA, beige) domain and a C-terminal Rec (Rec, violet) domain. The domains of ChpT are structurally related to the DHp and CA domains of CckA, although the latter is functionally degenerated. ChpT can phosphorylate two acceptors, the classical response regulator CtrA and the single-Rec protein CpdR. P~CtrA binds as a dimer to the origin of replication to inhibit replication initiation. In parallel, CpdR phosphorylation impedes binding of CpdR to the protease complex ClpXP, which would prime the protease for CtrA degradation.

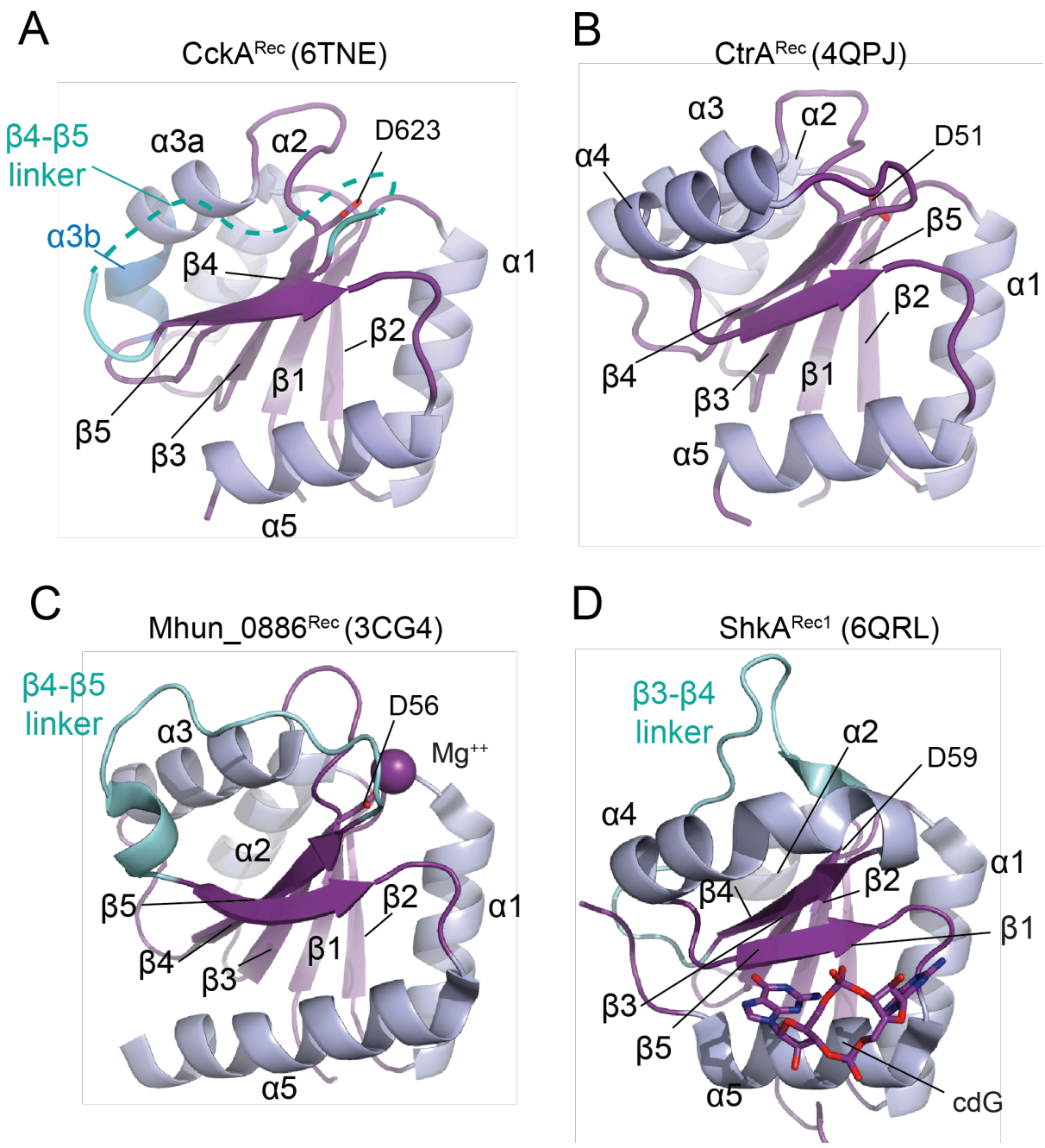

Figure 2. Structure comparison of CckA^{Rec} with the canonical fold of CtrA^{Rec}, and with other Rec domains lacking secondary structure elements. Cartoon representation with β-strands colored in purple and α-helices in light-blue. Non-canonical elements are indicated in cyan. PDB codes are given in brackets.

(A) CckA^{Rec} displaying the classical $(\beta\alpha)_5$. but with a disordered β4 - β5 linker instead of an α4 helix. Note, that α3 is broken into two pieces (α3a and α3b) as indicated by the difference in colouring.

(B) As reference, CtrA^{Rec} from *B. abortus* shows the canonical $(\beta\alpha)_5$ Rec fold.

(C) The β4 - β5 linker of receiver domain Mhun_0886^{Rec} exhibits irregular loop structure with a small helical section.

(D) The cryptic receiver domain ShkA^{Rec1} lacks α3 and binds cyclic-di-GMP that modulates the function of the full-length protein.

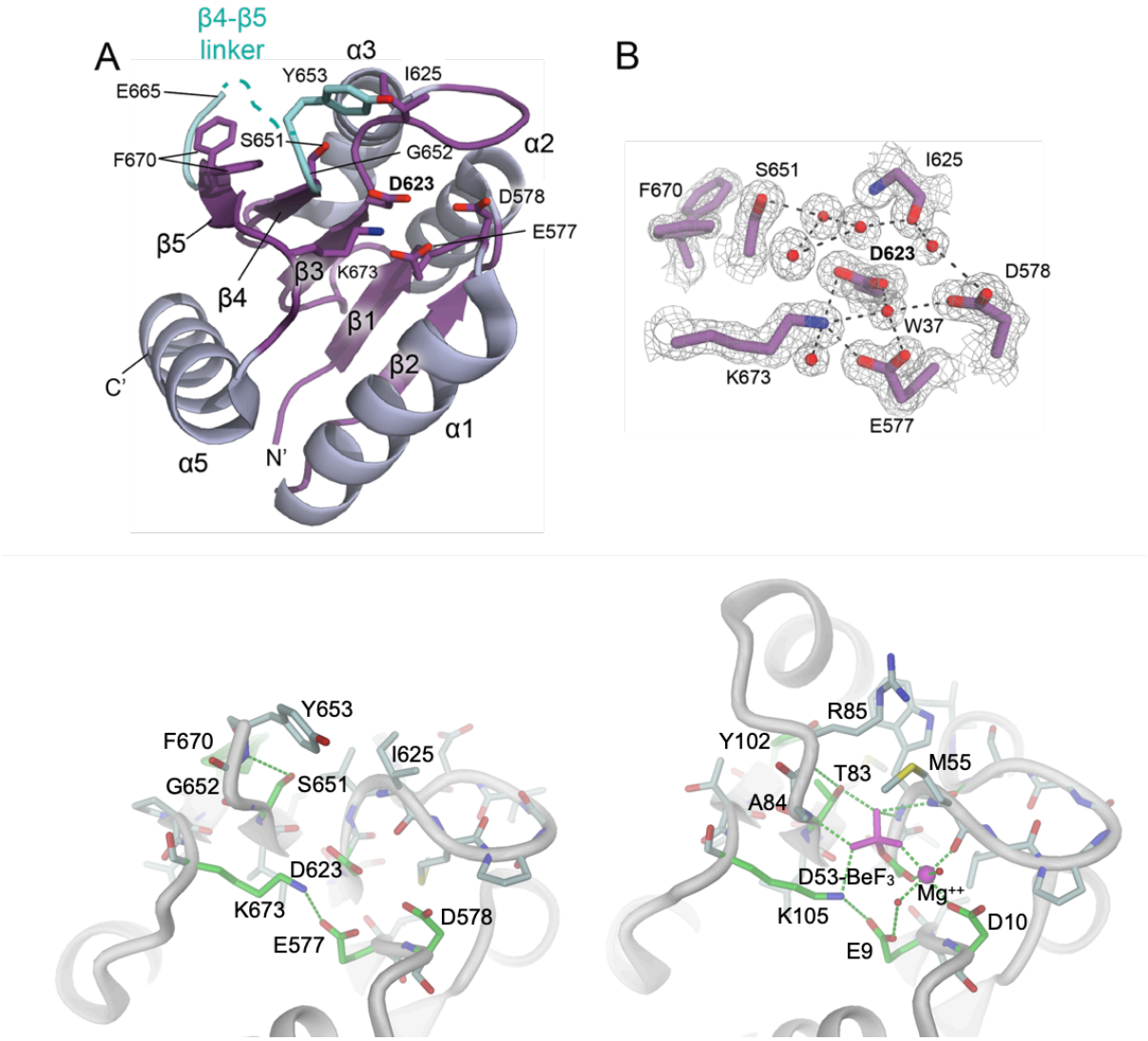

Figure 3. Crystal structure of CckA^{Rec}.
(A) Cartoon representation with β-strands colored in purple and α-helices in light-blue. CckA^{Rec} exhibits the canonical $(\beta\alpha)_5$ fold of response regulator receiver domains, but lacks on ordered α4 helix. The corresponding segment joining β4 - β5 is indicated in cyan. The phospho-acceptor D623, acidic pocket residues D578, E579, and K673 implicated in phosphoryl stabilization are shown in full. Also shown are S651 and F670 (with two alternative rotamers) implicated in conformational switching in canonical Rec domains.
(B) Detailed view of the phospho-acceptor site with 2Fo-Fc omit map contoured at 1.2 σ overlayed. Several water molecules are well resolved (red spheres) with W37 occupying the canonical Mg^{++} binding sites. Potential hydrogen bonds (<3.5 Å) are indicated by dashed lines.
(C-D) Full representation of active sites of CckA^{Rec} (C) and activated PhoB (D) with selected H-bond and coordination interactions indicated by green, stippled lines. Note that despite the absence of Mg^{++} and BeF_3^-, the active site of CckA^{Rec} is in the activated conformation. See also Figs. S3A,B.

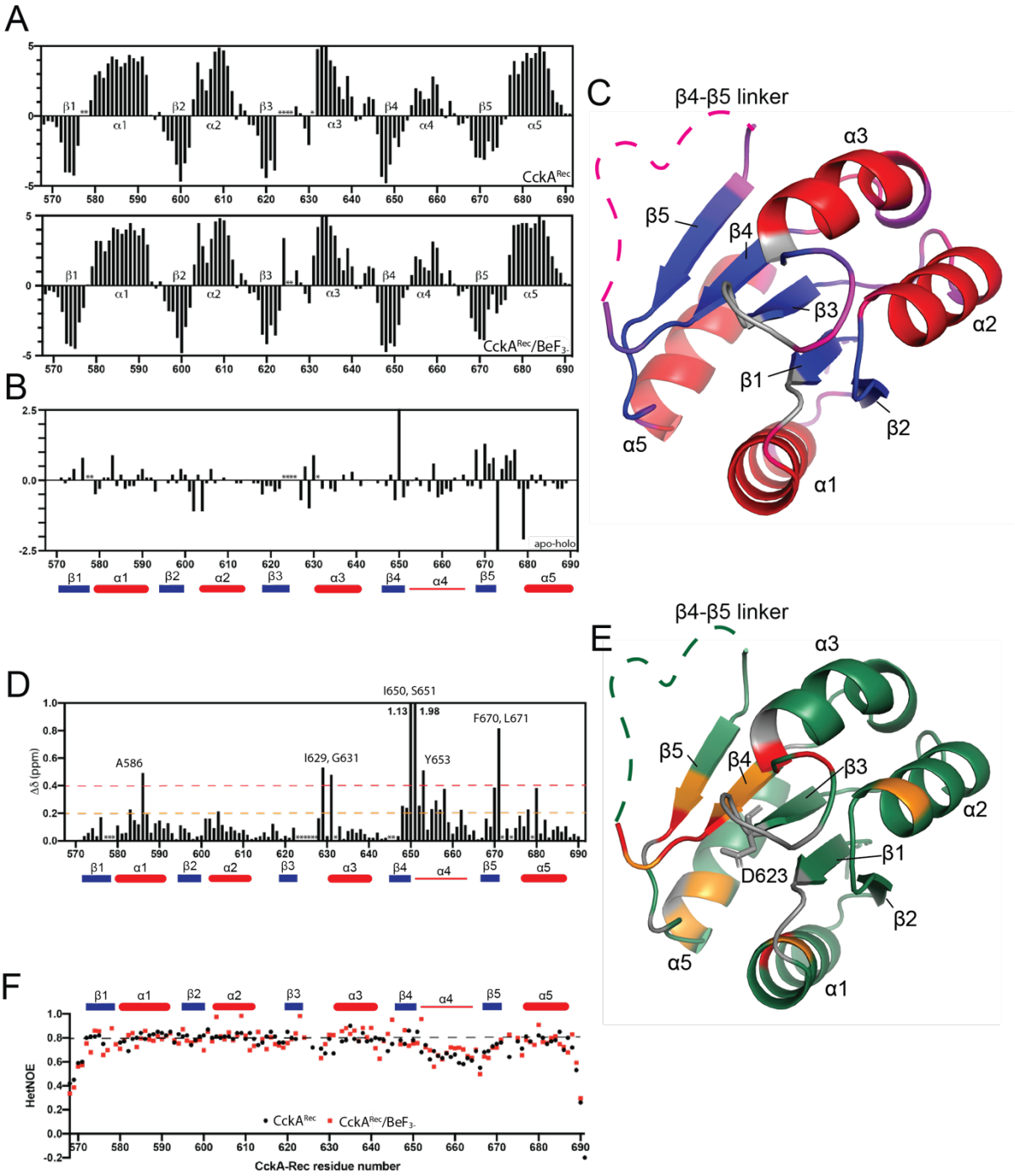

Figure 4. NMR data of apo and BeF_3-activated $CckA^{Rec}$.

(A) Sequence-specific secondary chemical shifts of apo $CckA^{Rec}$ (top) and BeF_3 activated $CckA^{Rec}$ (bottom) relative to the random coil values of Kjaergaard *et al.* Unassigned residues are marked with an asterisk.

(B) Sequence-specific secondary chemical shift difference between apo $CckA^{Rec}$ and activated $CckA^{Rec}$. Unassigned residues are marked with an asterisk.

(C): Structure of $CckA^{Rec}$ with the positions of secondary structure elements identified by NMR spectroscopy indicated by red (α -helices) and blue (β-strands). The β4-β5 loop and other parts

with weak positive α-helical propensity are plotted in pink onto the structure. Unassigned residues are shown in grey.

(D): Chemical shift perturbation of $CckA^{Rec}$ upon BeF_3 binding. Two significance levels of the chemical shift differences are indicated by the orange and red lines. Not assigned residues are marked with an asterisk.

(E): The two significance levels are plotted onto the structure of apo $CckA^{Rec}$ (orange: 0.2-0.4 ppm; red: > 0.4 ppm). Unassigned regions are colored in grey and the conserved aspartate D623 is labelled.

(F): Heteronuclear NOEs of apo $CckA^{Rec}$ (black) and activated $CckA^{Rec}$ (red). Secondary structures are indicated above the graph α -helices (beige), β-strands (purple) and α4 in red.

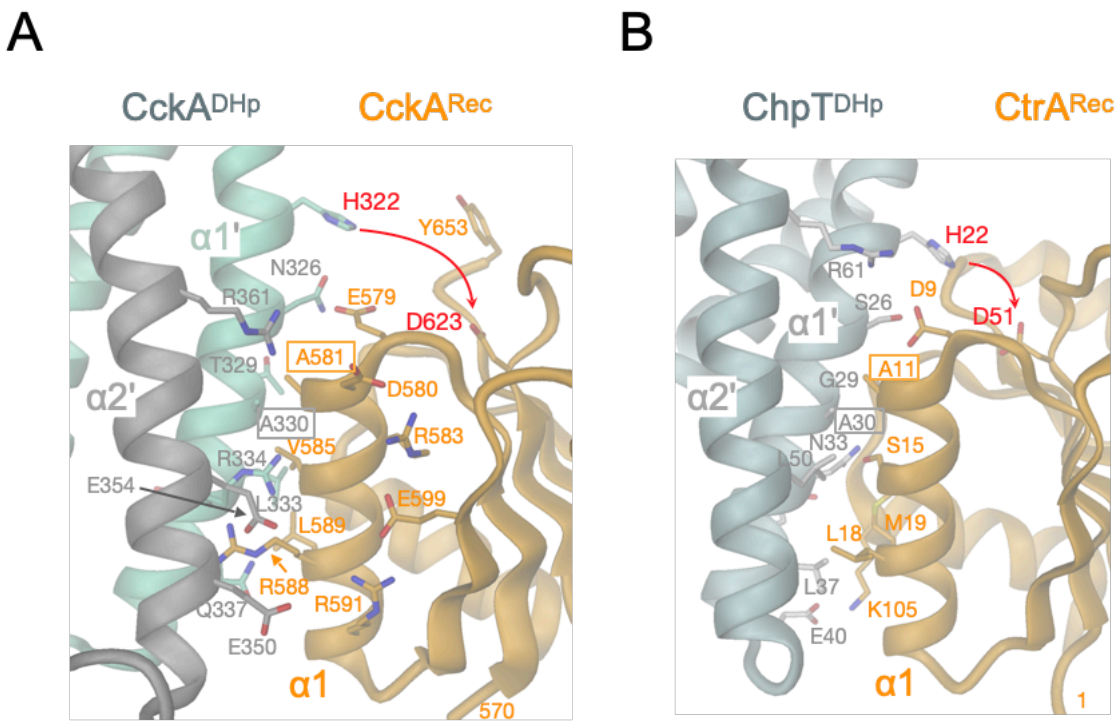

Figure 5. Phosphotransfer competent DHp / Rec association in HHKs. Cartoon representation (DHp, grey/aquamarine; Rec, orange) with interface residues shown in full. Active histidine and aspartate residues participating in the phosphotransfer are linked by a red arrow. Alanine interface residues, which are conserved between the depicted complexes, have boxed labels.
(A) Model of $CckA^{DHp}$/$CckA^{Rec}$ based on the structure shown in panel B. The two DHp helices interacting with Rec (α1', α2') are distinguised by color, since they belong to different subunits of the homodimer. Also shown residues of the intramolecular D580 - R593 - E599 - R591 network of $CckA^{Rec}$.
(B) Structure of $ChpT^{DHp}$/$CtrA^{Rec}$ (4QPJ). Note, that α1' and α2' of DHp belong to the same subunit, in contrast to the situation in CckA.

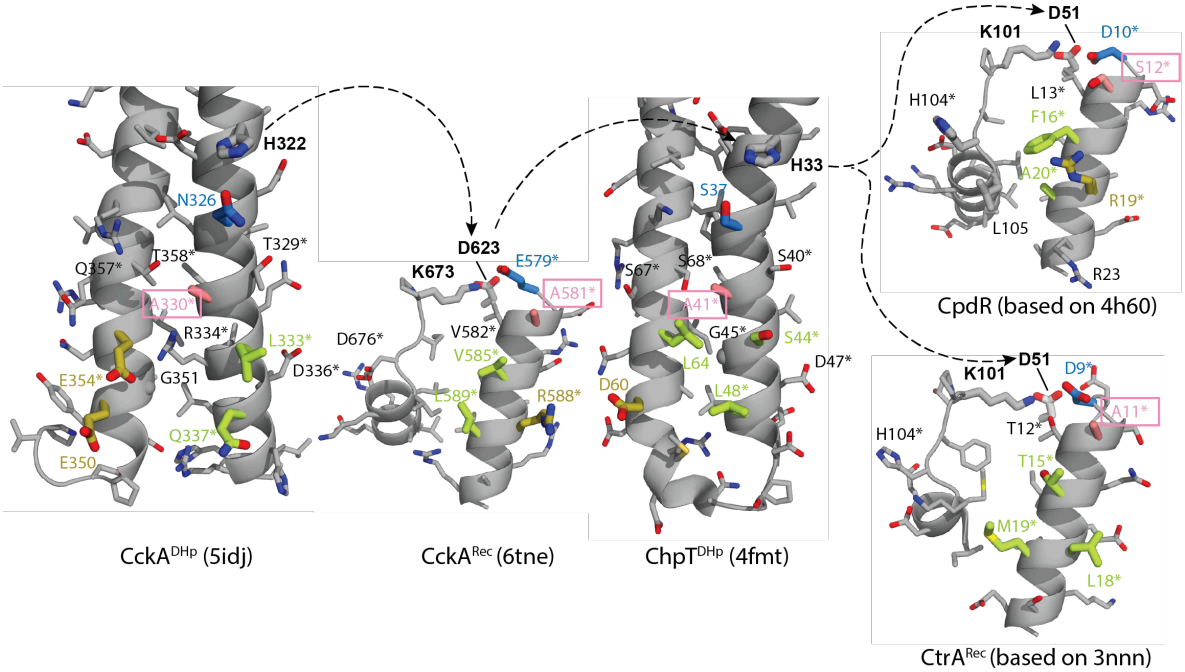

Figure 6. Openbook representation of protein interfaces of the CckA - ChpT - CtrA/CpdR phosphorelay of *C. crescentus*. On the left, the open book representation of the CckA DHp/Rec model (Fig. 5A) has interacting residues high-lighted by thick bonds and their carbon atoms colored according to individual subcontacts (blue, salmon, green, yellow). The (His-Asp-His-Asp) phosphoryl-transfer path between alternating DHp and Rec domains is indicated by broken arrows. Labels marked by * indicate positions that have been prediced to interact based on co-variation by Skerker et al., 2008). Note, that the two DHp domain of CckA and ChpT superimpose with a rmsd of 1.3 Å (43 Cα positions).

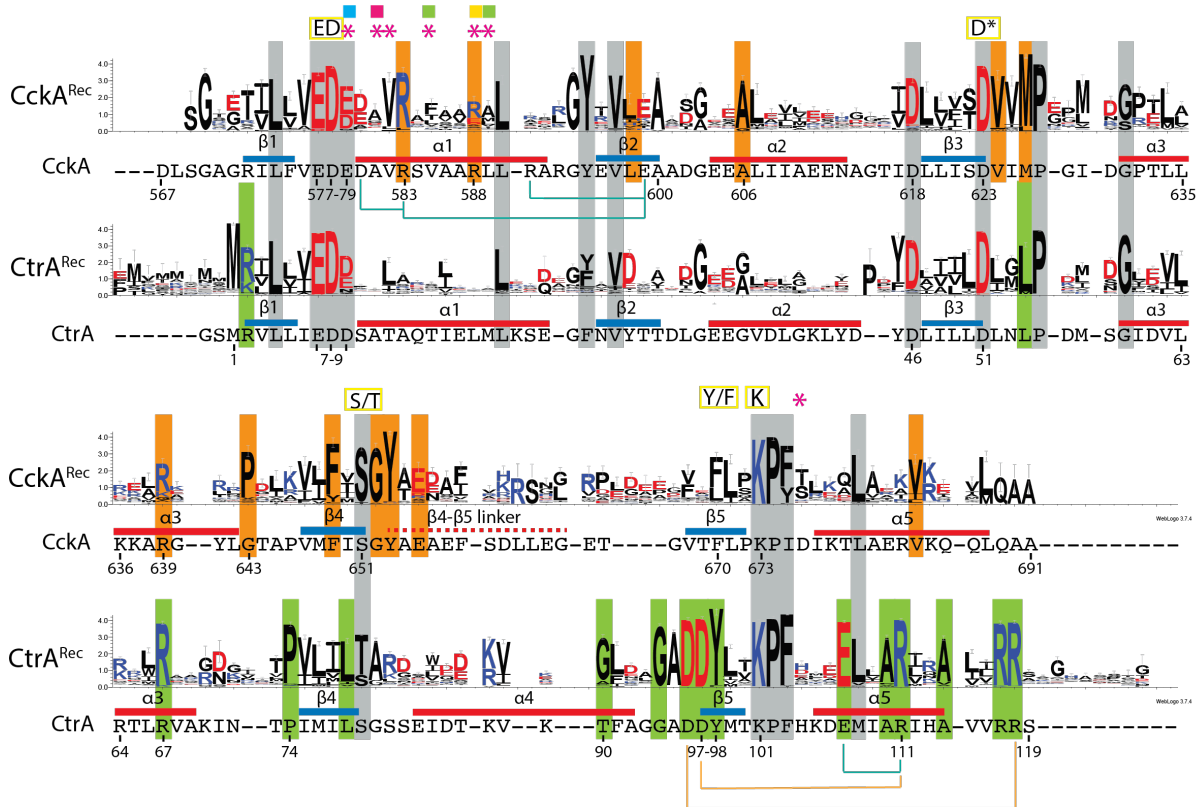

Figure 7. Comparison of CckA^Rec and CtrA^Rec sequence logos. Overall conserved residues are marked with grey background, whereas specifically conserved CckA^Rec or CtrA^Rec residues are marked with orange and green background, respectively. The relevant part of the CckA and CtrA sequences of *C. crescentus* are reproduced below the logos, with intra-domain salt-bridges indicated by light-blue lines. Also indicated are inter-domain salt-bridges (orange lines; see FigS3B) found in activated, dimeric CtrA^Rec structures. The quintet of functionally relevant residues (ED, D*, S/T, Y/F, K), residues co-evolving with cognate DHp domains (Skerker et al., 2008) (magenta asterisks), and residues of the sub-contact patches defined in Fig. 6 are marked on the top.

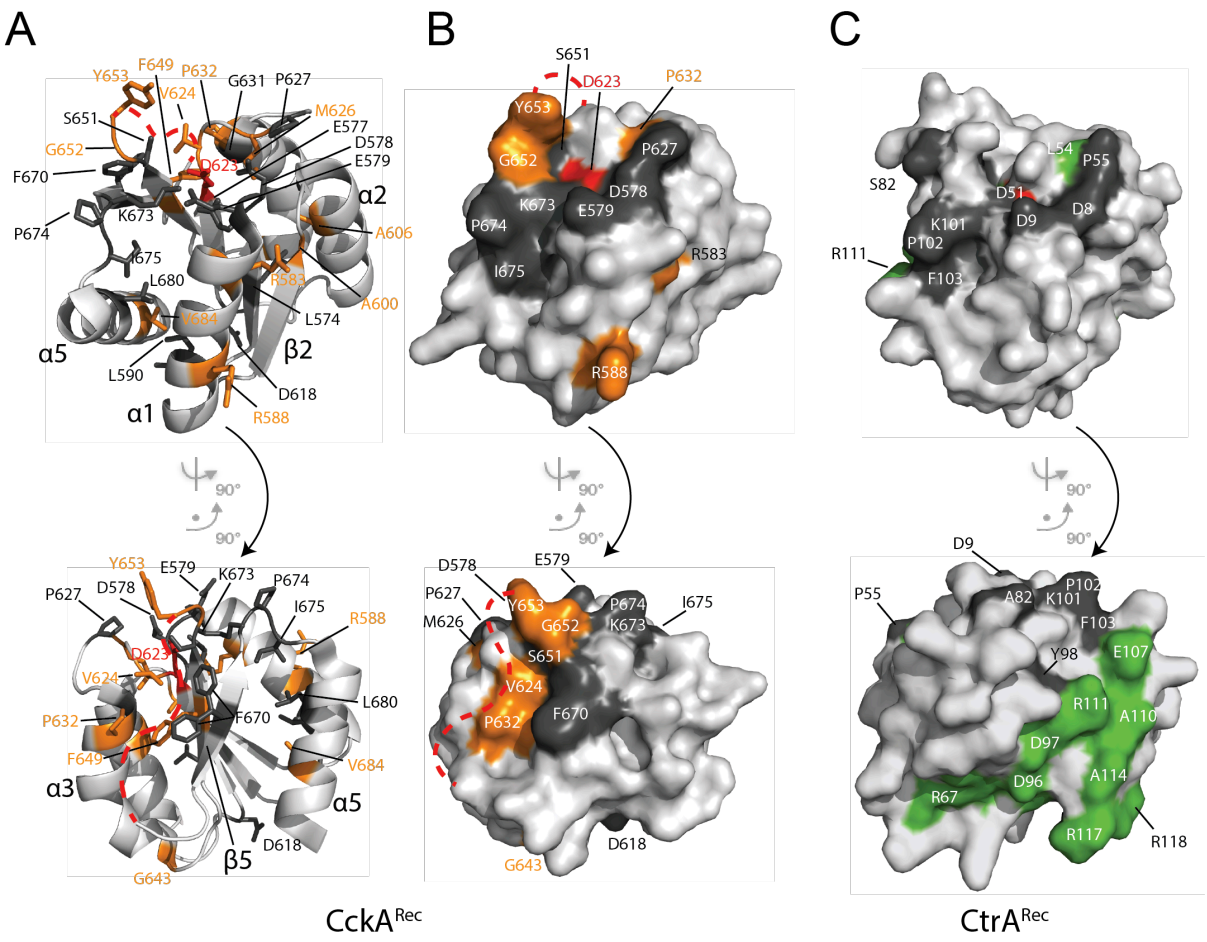

Figure 8. Residue conservation in CckA^{Rec} and CtrA^{Rec} mapped onto structures. (A) CckA^{Rec} in cartoon representation with conserved residues in full. (B, C) Surface representation of CckA^{Rec} and CtrA^{Rec} with conserved residues coloured according to Fig. 7 and the active aspartate in red. The disorered β4 - β5 linker of CckA^{Rec} is indicated by the red dashed line. The top row shows the view onto the α1 face, which would interact with DHp, the bottom row shows the view onto the 4-5-5 face, which is involved in dimerization in CtrA^{Rec} homologs.

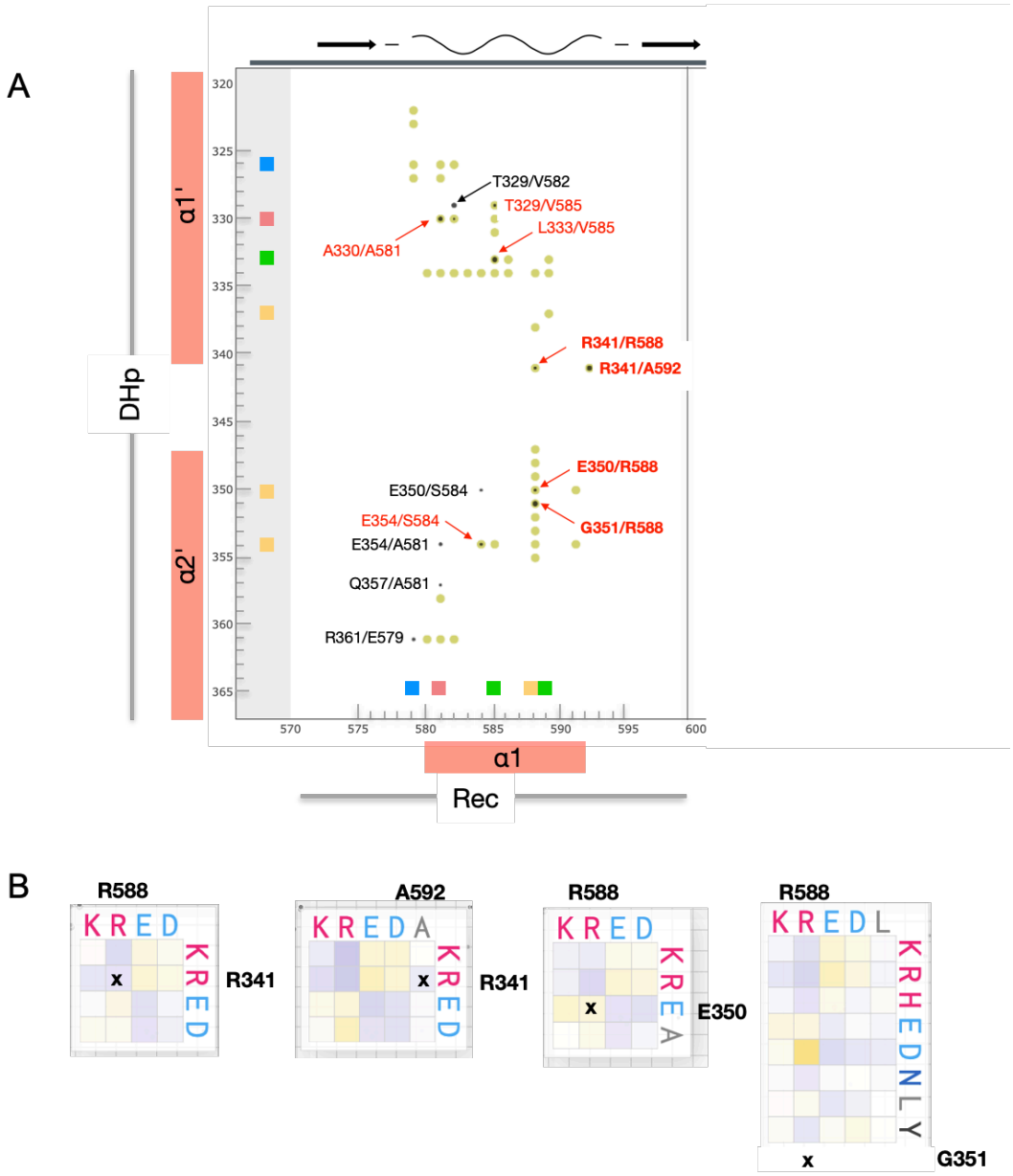

Figure 9. DHp / Rec contacts as revealed by co-variation analysis of HHK sequences.
(A) Co-variation scores above 3.0 between DHp (vertical axis) and part of Rec (horizontal axis) residues are shown as filled circles, with size proportional to signal strength. Residues of the sub-contact patches defined in Fig. 6 are indicated by correspondingly colored squares on the axes. Distances < 6 Å in the $CckA^{DHp}/CckA^{Rec}$ model (Fig. 5A) are indicated by filled yellow-green circles. The full co-variation matrix is given in Fig. S8. Co-variation peaks that correspond to close distances are labeled in black (< 8 Å) or red (< 6 Å). Contacts that constitute potential ion-pairs are labeled in bold with further information given in panel B.
(B) Substitution matrices for selected DHp / Rec residue pairs. Note that e.g. R341/A592 do not form a contact in the model (due to the short A592 side-chain), but position 592 is often occupied by a D or E.

Table 1. Crystallographic data collection and refinement statistics

Data collection	
Synchrotron source	SLS, PXI
Wavelength (Å)	1.00004
Space group	I 1 2 1
a, b, c (Å)	37.4, 42.9, 65.0
α, β, γ (°)	90.0, 94.4, 90.0
Resolution (Å)	28.2-1.25 (1.29-1.25)
No. of unique reflections	28065 (2818)
No of reflections used for R_{free}	1372 (136)
Completeness (%)	98.37 (99.58)
I/σ (I)	17.24 (4.96)
Redundancy	2.0 (2.0)
R_{merge} (%)	1.7 (12.9)
R_{pim} (%)	1.7 (12.9)
CC (1/2) (%)	99.9 (94.0)
Refinement	
R_{work}/R_{free} (%)	20.6/22.7
RMSD from ideal values	
-- Bond length (Å)	0.0123
-- Bond angles (°)	1.7
Molecules/asymmetric unit	1
No. of atoms	
-- Protein	839
-- Water	93
Average B-factor (Å^2)	18.9
-- Protein (Å^2)	17.5
-- Water (Å^2)	31.7
Ramachandran statistics	
-- Favored regions (%)	100.0
-- Allowed regions (%)	0.0
-- Disallowed regions (%)	0.0
PDB Code	6TNE

Supplementary Figures

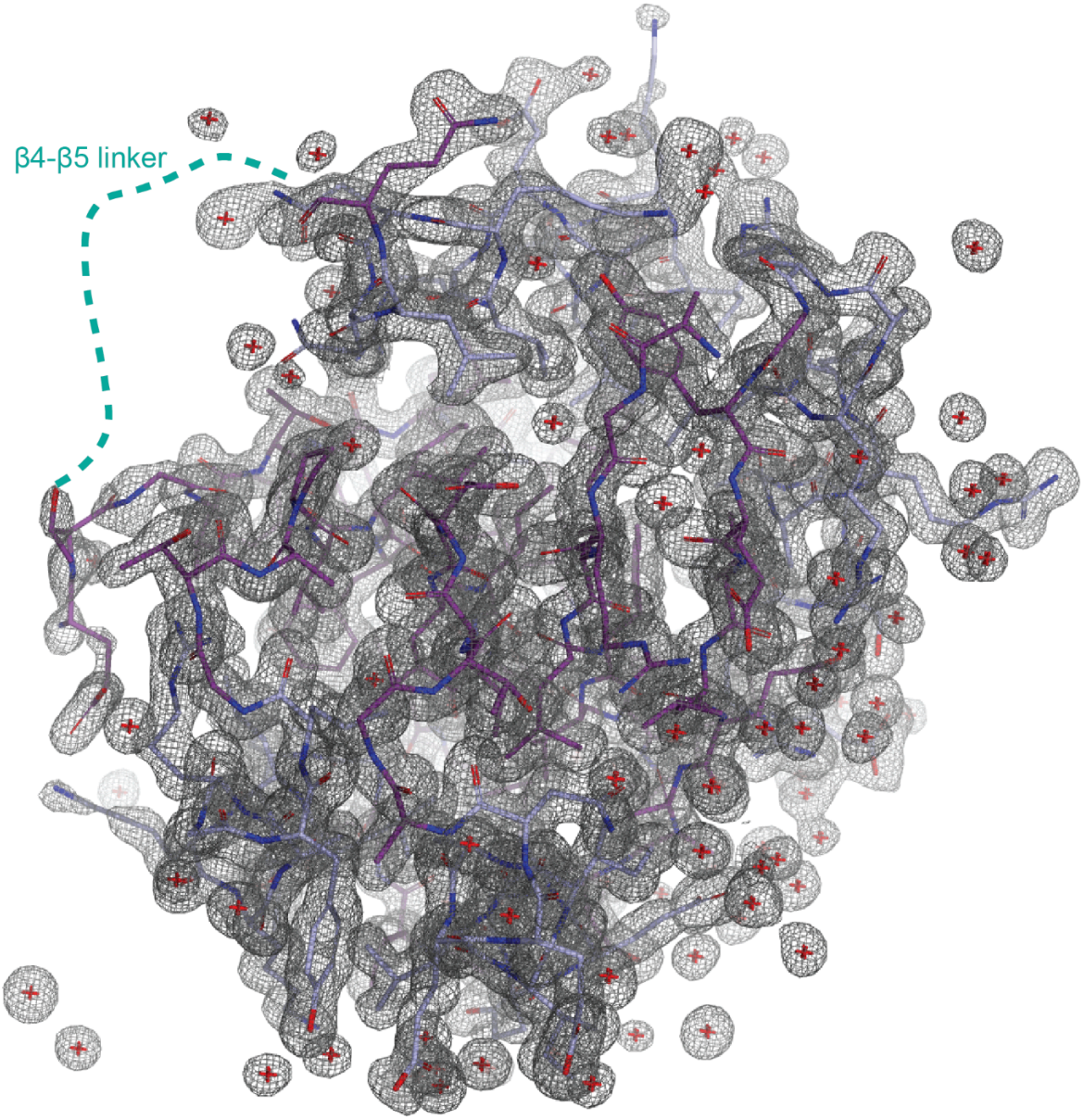

Supplementary Figure S1. Electron density and full model of CckA. The electron density is clearly defined for the entire molecule with the exception of the β4 - β5 linker. Water molecules are shown as red crosses.

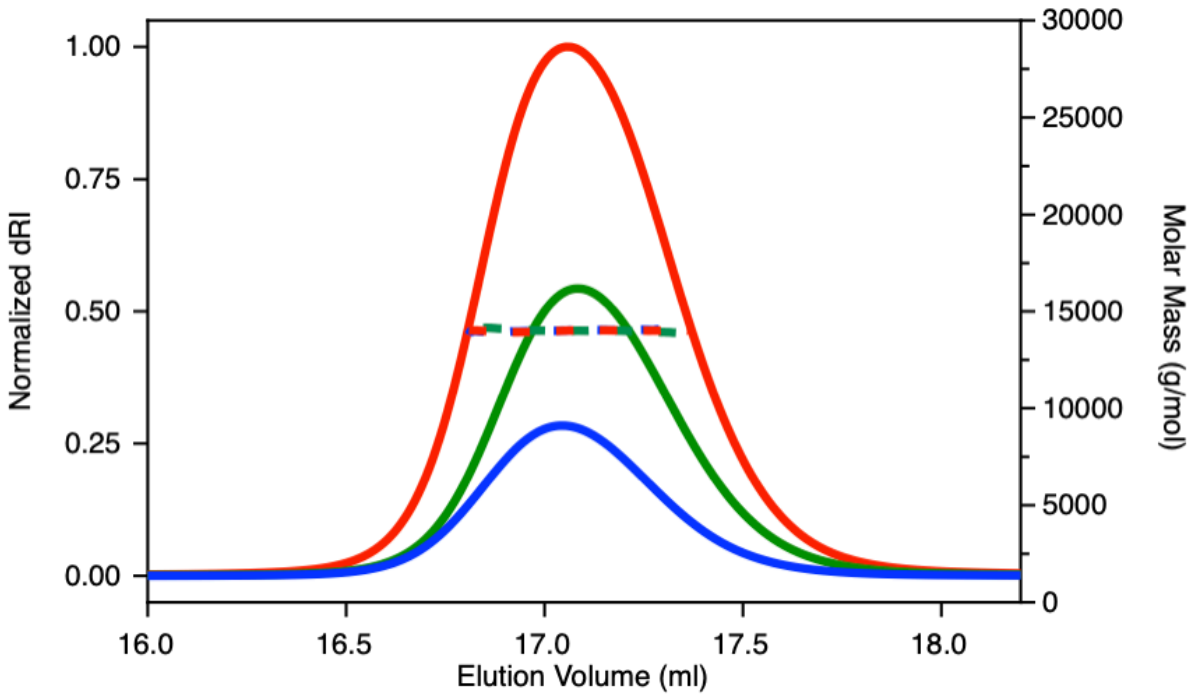

Supplementary Figure S2. SEC-MALS profile of CckA^{Rec}. Molecular mass values (right axis) are represented by dotted lines and change in refractive index (left axis) by solid lines. Protein concentrations are shown at the top right of the figure.

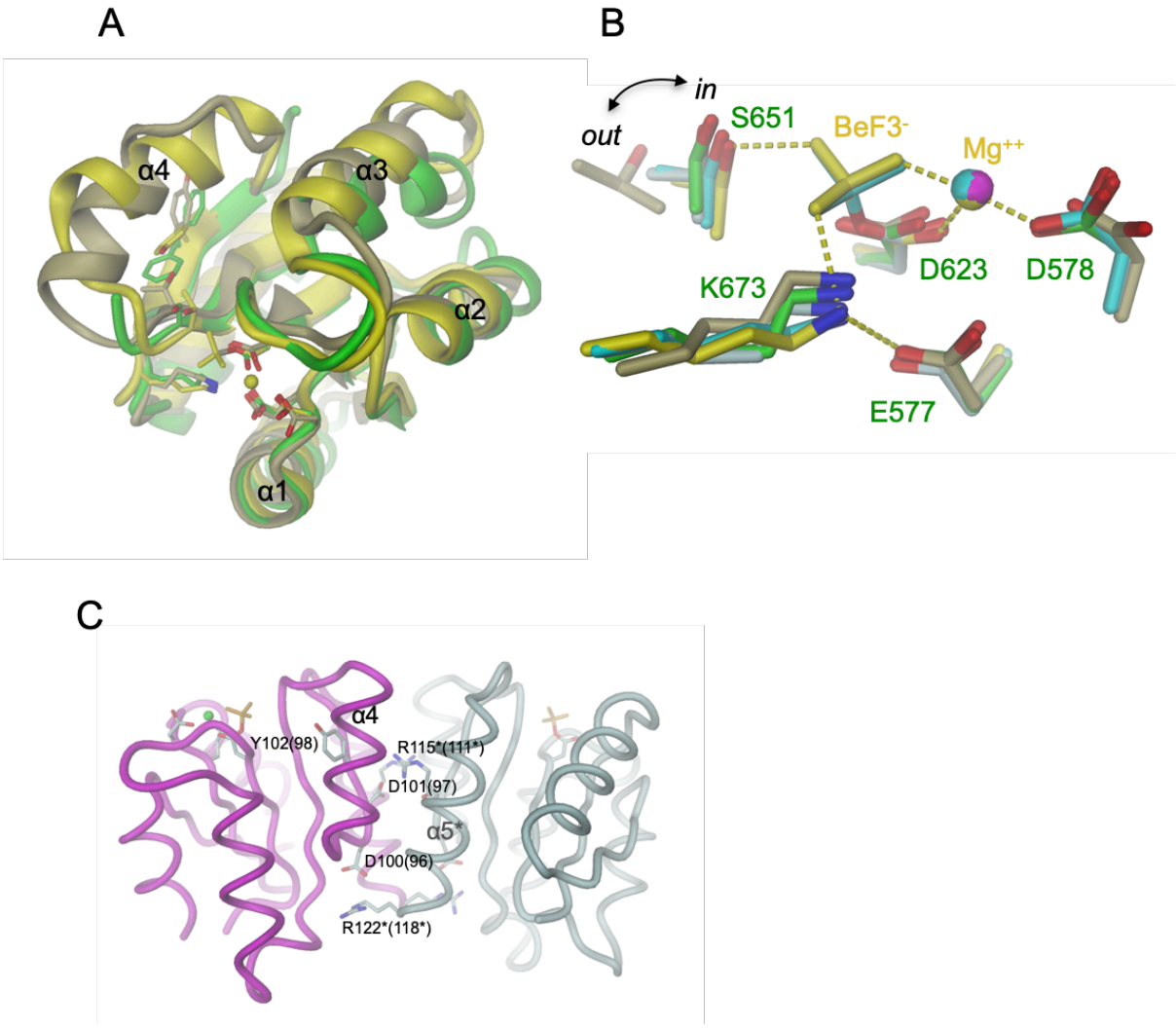

Supplementary Figure S3. Structure comparison of CckA^{Rec} with native and activated Rec domains.

(A) Superposition of CckA^{Rec} (green), native PhoB (1b00, khaki), and BeF_3^- modified PhoB (1zes, yellow). Residues of the active site and the Y/F residue of the switch are shown in full. Note that F670 of CckA^{Rec} exhibits two alternative conformations that coincide with the outward and inward orientation seen in native and activated PhoB, respectively. For the superposition, only the Cα - positions of the depicted residues except Y/F were used.

(B) Close-up of active sites shown in (A) together with those of native (6is2, white) and BeF_3^- modified ArlR (6is1, cyan). Note that all structures, including that of CckA^{Rec} (green) exhibit the same arrangement (activated conformation, rmsd = 0.40 - 0.58 Å for all atoms) with the exception of native PhoB (khaki), which has the S/T residue in an "out" position (rmsd = 0.77 Å).

(C) Dimeric structure of BeF_3^- modified PhoB (1zes) with selected residues, including conserved charged residues of the interface, in full. Asterisks indicate symmetry related residues. CtrA residue numbers are given in brackets.

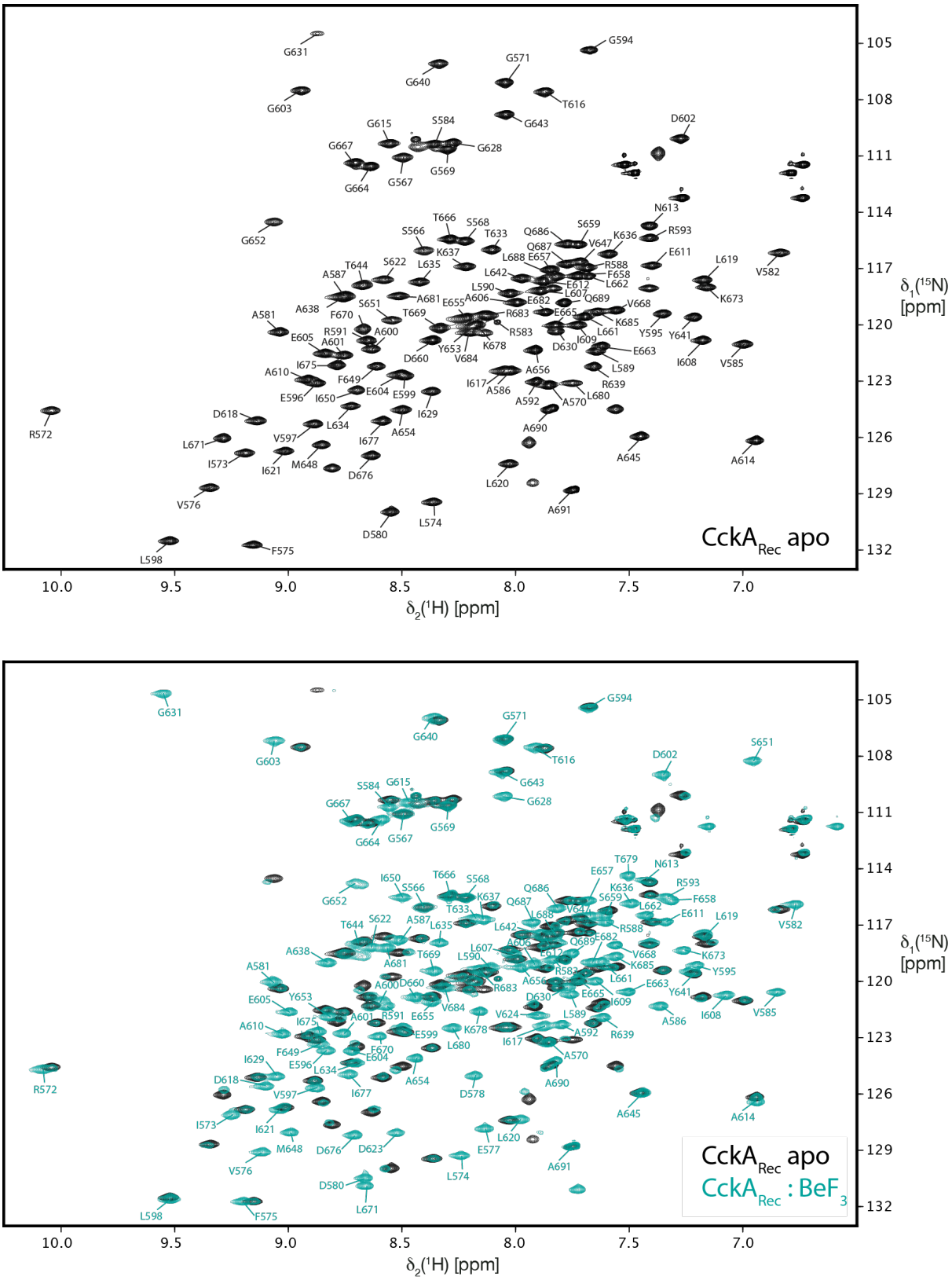

Supplementary Figure S4. NMR resonance assignments of apo and BeF_3-activated $CckA_{Rec}$. The top panel shows the 2D [^{15}N,^{1}H]-HSQC spectrum of 0.8 mM CckARec recorded at 25°C in 25 mM MES pH 6.8 with 100 mM NaCl and 5 mM $MgCl_2$ in 95%/5% H_2O/D_2O. The sequence-specific resonance assignments are indicated. The bottom panel shows the same NMR spectrum of apo $CckA_{Rec}$ as in the top panel (black resonances) overlaid with the 2D

[^{15}N,H]-HSQC spectrum of 0.4 mM CckA^{Rec} in the presence of 10 mM BeF_3 (bluegreen resonances). Sequence-specific resonance assignments are indicated for the higher populated activated BeF_3 bound state of CckA^{Rec}

A

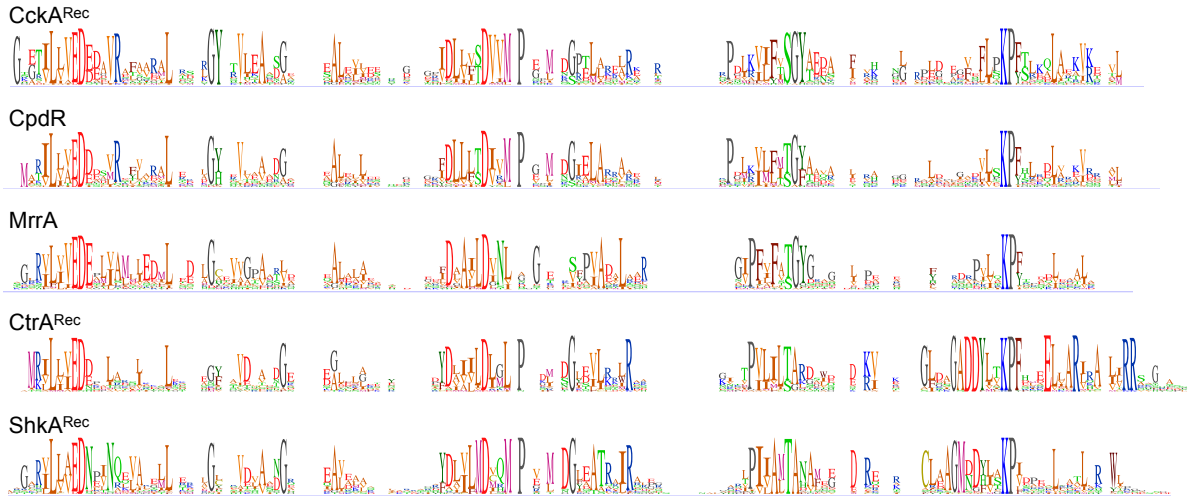

B

log(E) score of sequence/motif match

			Rec domain			HMM Rec motif				
organism	protein	UNIPROT	type	PDB	FATGUY motif	CckA^{Rec}	CpdR	MrrA	CtrA^{Rec}	ShkA^{Rec}
C. cresc	CckA	Q9X688	HHK	6tne	FISGYAE	-43	-33	-11	-16	-16
C. cresc	CpdR	Q9AA62	single		FITGFAA	-32	-49	-12	-20	-22
C. cresc	MrrA	Q9A428	single		FASGYGE	-14	-14	-49	-9	-10
C. cresc	CtrA	P0CAW8	RR			-19	-24	-13	-51	-24
C. cresc	ShkA	Q9ABT2	HHK *)	6qrj		-14	-20	-12	-27	-52
B. subtilis	Spo0F	P06628	single	2ftk	IMTAYGE	-26	-31	-17	-24	-24
R. meliloti	Sma011	Q930Y6	single	2lpm	FATGYGS	-15	-16	-47	-13	-11
S. melonis	SdrG	A0A0D1M	single	5ieb	FATGGSD	-10	-12	-44	-8	-6
P. aerug	PA1611	Q9I3B1	HHK	7c1j		-16	-22	-14	-29	-54
S. cerevisiae	SLN1	P39928	HHK	2r25		-14	-16	-6	-16	-37
A. thaliana	AHK5	Q3S4A7	HHK	4euk		-14	-18	-9	-17	-43
A. thaliana	CKI1	O22267	HHK	3mmn		-12	-12	-6	-13	-30
E. coli	RcsC	P0DMC5	HHK *)	2ayz		-22	-26	-11	-22	-35

Supplementary Figure S5. Sequence logos for five distinct Rec groups and correlation (E-values) of selected sequences against derived HMM motifs.
(A) Rec logos as derived from the alignment of homologous sequences retrieved by HMMER. The names of the founder sequences are indicated. For details see Material and Methods.
(B) HMMSCAN E-scores of full-length sequences against the HMM Rec motifs corresponding to the logos shown in (A). Orange background: E < 1e-40, dark grey: E < 1e-30, light grey:E < 1e-25. *): C-terminal domain of the two Rec domains.

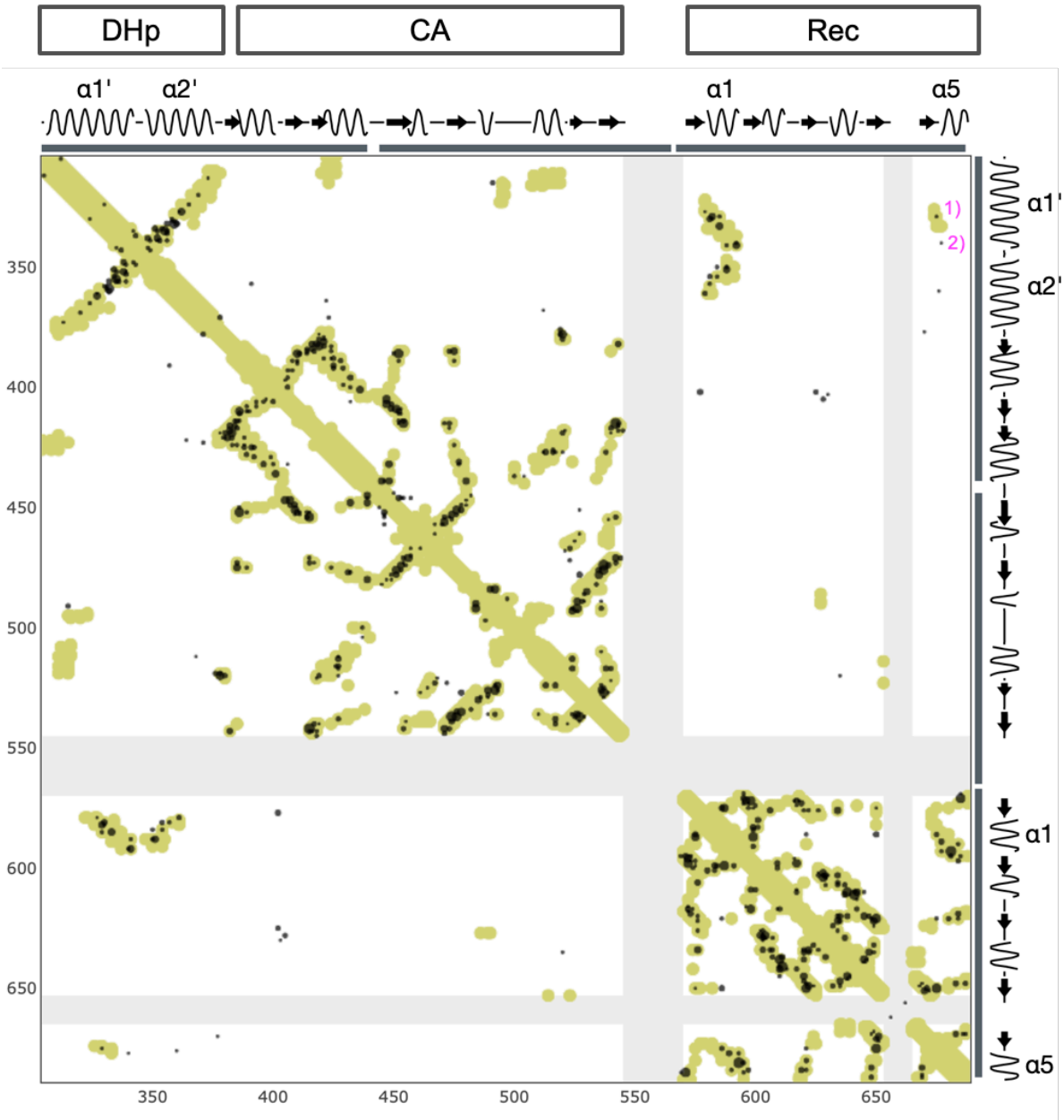

Supplementary Figure S6. HHK co-variation analysis. EVcoupling matrix based on 8067 sequences retrieved with CckA query sequence and an E-value of 1e-60. All peaks (scaled according to score) with a probability >95% are shown. Yellow dots indicate contacts with a distance < 6Å in the CA_DHp_Rec phosphotransfer model of CckA (Fig. 5). Some helices of the DHp domain (α1', α2') and the Rec domain (α1 to α2) are labeled on the axes. Significant Rec / DHp (top right part of the matrix) covariation values are found almost exclusively between Rec-α1 and the α1',α2' DHp helices (see the zoom-in of Fig. 9). The peaks marked with 1) and 2) correspond to T329/I675 and H340/I677 (distance 10 Å), respectively, and involve Rec β5-α5. All other inter-domain correlations are probably spurious or indirect, since all their distances are > 20 Å